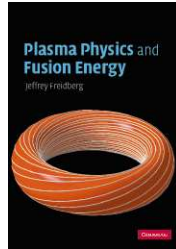


Cambridge Books Online

<http://ebooks.cambridge.org>



Plasma Physics and Fusion Energy

Jeffrey P. Freidberg

Book DOI: <http://dx.doi.org/10.1017/CBO9780511755705>

Online ISBN: 9780511755705

Hardback ISBN: 9780521851077

Paperback ISBN: 9780521733175

Chapter

8 - Single-particle motion in a plasma – guiding center theory pp. 139-182

Chapter DOI: <http://dx.doi.org/10.1017/CBO9780511755705.010>

Cambridge University Press

8

Single-particle motion – guiding center theory

8.1 Introduction

A major goal of this book is to provide an understanding of how magnetic fields confine charged particles in a fusion plasma. As such, one would like to develop an intuition about the detailed behavior of particle orbits in self-consistent magnetic fields. In particular, it must be demonstrated that charged particles stay confined within the plasma and do not become lost drifting across the field and hitting the first wall.

As a first step towards this goal this chapter focuses on the motion of charged particles in prescribed magnetic and electric fields. No attempt is made at self-consistency – for example, to include the currents and corresponding induced magnetic fields resulting from the flow of charged particles. The fields are simply specified as known quantities. They are assumed to be smooth, slowly varying functions in order to be compatible with the requirement that plasmas be dominated by long-range collective effects. The question of self-consistent fields is deferred to future chapters after appropriate models have been developed.

In the process of studying single-particle motion it will become apparent that there is a well-separated hierarchy of frequencies that characterize the different types of motion that can occur. The fastest and dominant behavior corresponds to gyro motion in which particles move freely along magnetic field lines and rotate in small circular orbits perpendicular to the magnetic field. This motion provides perpendicular confinement of charged particles and makes a toroidal geometry necessary in order to avoid parallel losses.

The next contribution to the hierarchy of frequencies involves slow spatial and time variations in the fields, which lead to important modifications of the basic gyro motion. This regime is known as “guiding center motion.” Of particular interest is the development of guiding center drifts (\mathbf{v}_g) across the magnetic field. These drifts are, in general, slow compared to the thermal speed ($|\mathbf{v}_g| \ll v_T$) but are nevertheless very important for several reasons. First, one must check the direction of \mathbf{v}_g to make sure that particles do not drift directly into the wall – they do not, although it is by no means obvious at the outset. Second, these drifts are largely responsible for the currents that flow in the plasma and are therefore essential for the ultimate development of self-consistent models.

The study of guiding center motion in slowly varying fields is the main topic of this chapter. Here, the key word is “slowly.” Guiding center theory exploits the assumptions

that the fields vary slowly in space with respect to the gyro radius and slowly in time with respect to the inverse gyro frequency. The primary motivation for the development of guiding center theory is that the theory provides the basic intuition necessary to understand particle confinement in fusion plasmas.

Continuing, the third regime in the hierarchy of frequencies is the Coulomb collision frequency ν_{Coul} . While such collisions are rare, they are nevertheless crucial for the understanding of magnetic confinement. The reason is that Coulomb collisions are the primary mechanism by which particles and energy diffuse across a magnetic field (ignoring for the moment plasma turbulence) thereby reducing confinement. Even though collisions are infrequent, $\nu_{\text{Coul}} \ll |\mathbf{v}_g|/r_L \equiv \omega_g$, they represent the first appearance of a physical mechanism that leads to confinement losses.

The last term in the hierarchy corresponds to nuclear fusion collisions, which unfortunately are very rare. These are basically hard-sphere collisions, which were discussed in Section 3.2. Fusion collisions have little direct effect on particle motion. Indirectly they affect plasma confinement through alpha particle heating and D–T fuel depletion.

In summary, the hierarchy of frequency scales is

$$\omega_c \gg \omega_g \gg \nu_{\text{Coul}} \gg \nu_{\text{fus}}. \quad (8.1)$$

This chapter describes gyro motion and then focuses on guiding center theory, which correspond to the first two terms in the hierarchy. Coulomb collisions are discussed in the next chapter.

This chapter is organized as follows. The discussion begins with the basic building block of magnetic fusion – gyro motion in a uniform, time independent magnetic field. The gyro orbits are derived exactly starting from Newton’s law and the Lorentz electromagnetic force.

Next, a sequence of modifications is made to the magnetic field to model more realistic magnetic geometries. For each modification, attention is focused on calculating the resulting guiding center drift. The analysis makes use of straightforward perturbation theory, which exploits the assumptions of slow space and time variation of the applied fields. This allows each guiding center drift to be calculated by superposition.

There are a number of drifts to include. First the $\mathbf{E} \times \mathbf{B}$ drift arising from perpendicular electric and magnetic fields is calculated. Although it may seem counter-intuitive at present, the non-zero electric field does not violate the plasma’s shielding ability and in fact this drift is mandatory in order for the shielding effect to be maintained. Next, perpendicular gradients in a straight magnetic field are introduced leading to the ∇B drift. Following this, the straight field assumption is relaxed. It is shown that the curvature of a magnetic field leads to a drift appropriately known as the curvature drift.

The next modification is time dependence in both the magnetic and electric field. The dominant effect is the development of an inertia-driven drift, known as the polarization drift. The final modification involves gradients parallel to the magnetic field. This generates a parallel mirroring force that tends to keep particles with a high perpendicular velocity

confined between regions of high magnetic field and gives rise to the mirror concept. However, while the mirroring force improves parallel confinement, in the end collisions destroy the effect and the need for toroidicity persists.

The descriptions above indicate that there are a substantial number of modifications to include, and one may wonder whether or not the list is complete. In terms of the guiding center drifts the list is indeed complete – there are no additional guiding center drifts within the order to which the theory is carried out.

The main conclusion from this chapter is that a magnetic field can quite effectively confine charged particles in the perpendicular direction. There is no long-time confinement parallel to the field and this leads to the requirement for a toroidal geometry. While a number of slower cross-field particle drifts do develop because of modifications and additions to the constant, uniform magnetic field, the direction of these drifts does not lead to a flow of particles directly to the first wall. In terms of fusion, guiding center theory predicts good confinement of charged particles for a wide range of toroidal magnetic geometries.

8.2 General properties of single-particle motion

The development of guiding center theory begins with a discussion of several general properties of single-particle motion in magnetic and electric fields. Included in the discussion are the statement of the exact equations of motion to be solved and the derivation of general conservation laws leading to the identification of exact constants of the motion.

8.2.1 Exact equations of motion

The starting point for the development of guiding center theory is the exact equations of motion as determined from Newton's law. For plasma physics applications only the magnetic and electric forces, given by the Lorentz force are required. Gravity is a very small effect and can be neglected. The equations to be solved are thus

$$\begin{aligned} m \frac{d\mathbf{v}}{dt} &= q(\mathbf{E} + \mathbf{v} \times \mathbf{B}), \\ \frac{d\mathbf{r}}{dt} &= \mathbf{v}. \end{aligned} \tag{8.2}$$

In general, $\mathbf{B} = \mathbf{B}(\mathbf{r}, t)$ and $\mathbf{E} = \mathbf{E}(\mathbf{r}, t)$ are functions of three dimensions plus time. Equation (8.2) is thus a set of coupled, non-linear, ordinary differential equations for the unknowns \mathbf{v} and \mathbf{r} as functions of t . They will be solved for a wide variety of cases by exploiting the underlying assumptions of guiding center theory, namely that the spatial variations of \mathbf{B} and \mathbf{E} occur on a length scale long compared to a gyro radius and that time variations occur on a time scale slow compared to the inverse gyro frequency.

8.2.2 General conservation relations

Several general conservation relations can be derived from Eq. (8.2). These involve the conservation of energy and momentum. When applicable the conservation relations lead to “exact constants of the motion,” which strongly constrain the particle’s orbit.

Consider first the situation in which $\mathbf{E} = 0$ and \mathbf{B} is independent of time: $\mathbf{B} = \mathbf{B}(\mathbf{r})$. Forming the dot product of Eq. (8.2) with \mathbf{v} leads to

$$m \mathbf{v} \cdot \frac{d\mathbf{v}}{dt} = \frac{d}{dt} \left(\frac{1}{2} m v^2 \right) = 0 \quad (8.3)$$

or

$$\frac{1}{2} m v^2 = \text{const.} \quad (8.4)$$

The conclusion is that the kinetic energy of a particle in a static magnetic field is a constant. In other words, a static magnetic field can do no work on a charged particle. Another basic related result is that a static magnetic field produces no force parallel to \mathbf{B} , a result that follows trivially from the relation $\mathbf{B} \cdot (\mathbf{v} \times \mathbf{B}) = 0$.

This relation can be generalized to include a static electric field. Since the fields are assumed static, Faraday’s law implies that $\mathbf{E}(\mathbf{r}) = -\nabla\phi(\mathbf{r})$. The dot product of Eq. (8.2) with \mathbf{v} is again formed. One now makes use of the identity (for a static field)

$$\frac{d\phi}{dt} = \frac{\partial\phi}{\partial t} + \mathbf{v} \cdot \nabla\phi = \mathbf{v} \cdot \nabla\phi, \quad (8.5)$$

from which it immediately follows that

$$W \equiv \frac{1}{2} m v^2 + q\phi = \text{const.} \quad (8.6)$$

The sum of kinetic and potential energy is a constant.

A simple prescription exists for the determination of exact constants of the motion. In general the fields are functions of x, y, z, t . Consider the special cases where one or more of these variables is ignorable (i.e., the fields do not depend on these variables). For each ignorable variable, there is one exact constant of the motion. The time independent case above led to the conservation of energy. As another example assume the fields are independent of the coordinate y but not x, z, t . Introduce the scalar and vector potential in the usual way: $\mathbf{E} = -\nabla\phi - \partial\mathbf{A}/\partial t$ and $\mathbf{B} = \nabla \times \mathbf{A}$. Forming the dot product of the momentum equation with \mathbf{e}_y leads to

$$\begin{aligned} \frac{d}{dt} m v_y &= q(E_y - v_x B_z + v_z B_x) \\ &= -q \left(\frac{\partial A_y}{\partial t} + \frac{dx}{dt} \frac{\partial A_y}{\partial x} + \frac{dz}{dt} \frac{\partial A_y}{\partial z} \right) \\ &= -q \frac{dA_y}{dt}, \end{aligned} \quad (8.7)$$

where in the last step use has been made of the fact that $\partial A_y / \partial y = 0$. It thus follows that

$$p_y \equiv mv_y + qA_y = \text{const.} \quad (8.8)$$

The quantity p_y is the y component of canonical momentum. In a similar way it can be shown (see Problem 8.1) that in a cylindrical geometry with azimuthal symmetry (i.e., $\partial/\partial\theta = 0$) the θ component of canonical angular momentum is also a constant of the motion:

$$p_\theta \equiv mrv_\theta + qrA_\theta = \text{const.} \quad (8.9)$$

The existence of exact constants of the motion often proves useful in understanding the behavior of particle motion in complex electric and magnetic fields. In the discussion that follows, relatively simple forms for \mathbf{B} and \mathbf{E} are chosen that allow for a complete analytic solution of the particle orbits, and that explicitly demonstrate the existence of exact constants of motion.

8.3 Motion in a constant \mathbf{B} field

The basic building block of magnetic confinement is the behavior of a charged particle in a uniform, time independent, magnetic field. The orbit of such a particle exhibits good confinement perpendicular to the direction of the magnetic field and no confinement parallel to the magnetic field. This behavior can be explicitly demonstrated by solving Newton's laws of motion assuming $\mathbf{E} = 0$ and $\mathbf{B} = B\mathbf{e}_z$, where $B = \text{const.}$

In component form, the full set of Newton's laws reduces to

$$\begin{aligned} dv_x/dt &= \omega_c v_y & v_x(0) &= v_{x0} \equiv v_\perp \cos \phi, \\ dv_y/dt &= -\omega_c v_x & v_y(0) &= v_{y0} \equiv v_\perp \sin \phi, \\ dv_z/dt &= 0 & v_z(0) &= v_{z0} \equiv v_\parallel, \\ dx/dt &= v_x & x(0) &= x_0, \\ dy/dt &= v_y & y(0) &= y_0, \\ dz/dt &= v_z & z(0) &= z_0. \end{aligned} \quad (8.10)$$

Here $\omega_c = qB/m$ is the gyro frequency (sometimes also called the cyclotron or Larmor frequency) and v_\perp , ϕ , v_\parallel , x_0 , y_0 , z_0 are constants representing the initial velocity and position of the particle.

8.3.1 Parallel motion

Focus first on the motion parallel to the field. The relevant subset of equations is

$$\begin{aligned} dv_z/dt &= 0 & v_z(0) &= v_{z0} \equiv v_\parallel, \\ dz/dt &= v_z & z(0) &= z_0. \end{aligned} \quad (8.11)$$

The solution is easily found and is

$$\begin{aligned} v_z(t) &= v_\parallel, \\ z(t) &= z_0 + v_\parallel t. \end{aligned} \quad (8.12)$$

The behavior corresponds to a constant uniform motion. There are no parallel forces providing confinement and particles simply proceed unimpeded. The motion is therefore unconfined along a given magnetic line.

8.3.2 Perpendicular motion

In the x, y plane the force is always perpendicular to \mathbf{v} . Intuition from classical mechanics suggests that this will lead to a circular-type motion and this is indeed the case. Consider first the relevant equations for the velocity:

$$\begin{aligned} dv_x/dt &= \omega_c v_y & v_x(0) &= v_{x0} \equiv v_{\perp} \cos \phi, \\ dv_y/dt &= -\omega_c v_x & v_y(0) &= v_{y0} \equiv v_{\perp} \sin \phi. \end{aligned} \quad (8.13)$$

Eliminating v_x yields

$$\begin{aligned} d^2 v_y/dt^2 + \omega_c^2 v_y &= 0, \\ v_y(0) &= v_{\perp} \sin \phi, \\ dv_y(0)/dt &= -\omega_c v_x(0) = -\omega_c v_{\perp} \cos \phi. \end{aligned} \quad (8.14)$$

Equation (8.14) is a linear, ordinary differential equation with constant coefficients. Its general solution is easily found, and applying the initial conditions leads to

$$\begin{aligned} v_y(t) &= -v_{\perp} \sin(\omega_c t - \phi), \\ v_x(t) &= v_{\perp} \cos(\omega_c t - \phi). \end{aligned} \quad (8.15)$$

Observe that the particles rotate with an angular frequency equal to the gyro frequency. Also, for a uniform magnetic field, not only is the total kinetic energy conserved, but the separate parallel and perpendicular energies are individually conserved: $v_z^2(t) = v_{\parallel}^2 = \text{const.}$ and $v_x^2(t) + v_y^2(t) = v_{\perp}^2 = \text{const.}$

The solution for the perpendicular motion is completed by integrating the velocity, yielding expressions for the particle trajectory $x(t)$, $y(t)$. One obtains

$$\begin{aligned} x(t) &= x_g + r_L \sin(\omega_c t - \phi), \\ y(t) &= y_g + r_L \cos(\omega_c t - \phi). \end{aligned} \quad (8.16)$$

Here, the gyro radius (sometimes called the Larmor radius) is given by $r_L = v_{\perp}/\omega_c = mv_{\perp}/qB$. The quantities x_g , y_g are defined as the guiding center position of the particle:

$$\begin{aligned} x_g &\equiv x_0 + r_L \sin \phi, \\ y_g &\equiv y_0 - r_L \cos \phi. \end{aligned} \quad (8.17)$$

This nomenclature is motivated by the trajectory relationship

$$(x - x_g)^2 + (y - y_g)^2 = r_L^2, \quad (8.18)$$

which is illustrated in Fig. 8.1. Observe that the orbit of the particle is circular with a radius equal to the gyro radius. The center of the orbit is located at x_g , y_g and hence the

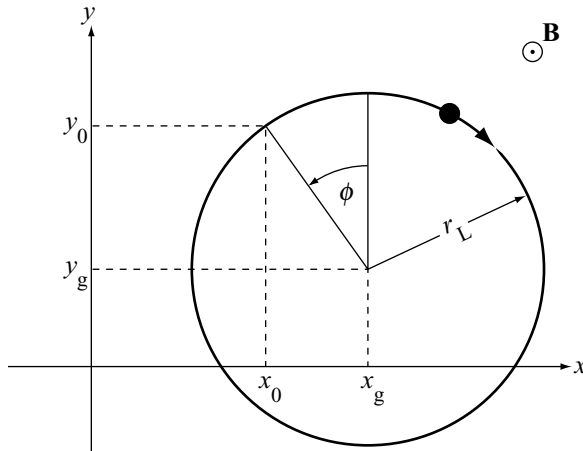


Figure 8.1 Gyro orbit of a positively charged particle in a magnetic field. Shown are the guiding center x_g, y_g and the initial position x_0, y_0 .

name “guiding center.” Since the gyro radius is, in general, quite small in comparison to the plasma radius, one can conclude that there is good confinement perpendicular to the magnetic field.

The concept of the guiding center is, as its name implies, the basis for “guiding center theory.” By following the velocity and position of the guiding center for more general fields one obtains an accurate picture of the average particle location, differing from the exact orbit by only a small deviation of order of the gyro radius. Guiding center motion indeed provides a powerful intuition into the motion of charged particles in slowly varying magnetic and electric fields, a very common practical situation.

A further property of gyro motion is the direction of rotation. Because the electrons and ions have opposite sign charges, they rotate in opposite directions. The actual rotation direction is determined in Fig. 8.2 by calculating the direction of the force $\pm |q| \mathbf{v} \times \mathbf{B}$. An easy way to remember the rotation direction is to note that the magnetic field generated by the electric current of a gyrating particle always opposes the applied magnetic field; that is, the gyro motion is diamagnetic. The sign of the charge can be easily taken into account in the description of gyro motion by defining the gyro frequency and gyro radius to always be positive, $\omega_c = |q| B/m$, $r_L = mv_{\perp}/|q| B$, and rewriting the solutions as follows:

$$\begin{aligned}
 v_x(t) &= v_{\perp} \cos(\omega_c t \pm \phi), \\
 v_y(t) &= \pm v_{\perp} \sin(\omega_c t \pm \phi), \\
 x(t) &= x_g + r_L \sin(\omega_c t \pm \phi), \\
 y(t) &= y_g \mp r_L \cos(\omega_c t \pm \phi),
 \end{aligned}
 \tag{8.19}$$

where the upper sign corresponds to a negative charge. Hereafter, the oscillating parts of these solutions is abbreviated to $\mathbf{v}_{\text{gyro}}(t)$ and $\mathbf{r}_{\text{gyro}}(t)$.

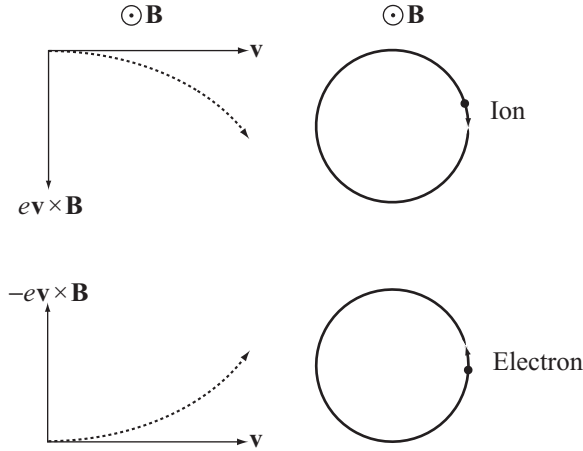


Figure 8.2 Force on a charged particle showing that the rotation is in the diamagnetic direction. For ions $q = +e$, while for electrons $q = -e$.

Lastly, consider the scaling consequences of gyro motion. Note that the gyro frequency increases with the magnetic field B : high $B \rightarrow$ high ω_c . Also the electron gyro frequency is much larger than the ion gyro frequency by the ratio m_i/m_e . The gyro radius increases with the perpendicular velocity v_\perp and decreases as the magnetic field B increases: high v_\perp , low $B \rightarrow$ large r_L . For a typical thermal particle with $v_\perp = v_T \equiv (2T/m)^{1/2}$ the ion gyro radius is larger than the electron gyro radius by the ratio $(m_i/m_e)^{1/2}$. Typical numerical values have been given in Chapter 7 and are repeated here for convenience:

$$\begin{aligned}
 \omega_{ce} &= \frac{eB}{m_e} = 1.76 \times 10^{11} B = 8.8 \times 10^{11} \text{ s}^{-1}, \\
 \omega_{ci} &= \frac{eB}{m_i} = 4.79 \times 10^7 B = 2.4 \times 10^8 \text{ s}^{-1}, \\
 r_{Le} &= \frac{(2m_e T_e)^{1/2}}{eB} = 1.07 \times 10^{-4} \frac{T_k^{1/2}}{B} = 8.3 \times 10^{-5} \text{ m}, \\
 r_{Li} &= \frac{(2m_i T_i)^{1/2}}{eB} = 6.46 \times 10^{-3} \frac{T_k^{1/2}}{B} = 5.0 \times 10^{-3} \text{ m}.
 \end{aligned}
 \tag{8.20}$$

These values correspond to $T_k = 15 \text{ keV}$, $B = 5 \text{ T}$, and a deuterium mass.

8.3.3 Consequences of gyro motion

The combined perpendicular and parallel motion of a charged particle corresponds to a helical trajectory as shown in Fig. 8.3. Particles spiral unimpeded along field lines with a small perpendicular excursion equal to the gyro radius. This has important implications for the geometry of a magnetic fusion reactor. Specifically, the magnetic geometry must be toroidal. A technologically simpler, linear geometry does not work, as shown in Fig. 8.4(a).

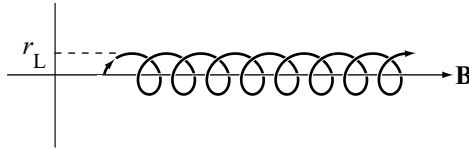


Figure 8.3 Helical trajectory of a charged particle in a uniform magnetic field.

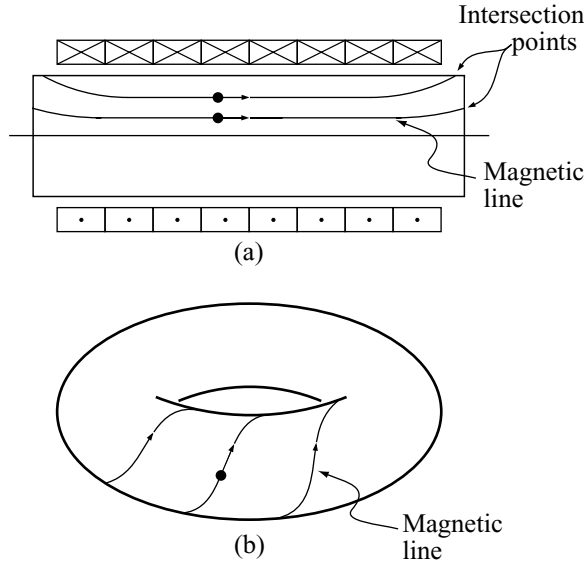


Figure 8.4 (a) Particles streaming along a magnetic line and being lost as they collide with the wall. (b) Magnetic lines wrapping around a torus preventing free streaming end loss.

Observe that in a finite length linear geometry all magnetic field lines must eventually make contact with the first wall as they leave the system. The particles therefore free stream along the field lines directly colliding with the wall in a very short time. In other words, the particles are not confined and there is no time for fusion reactions to occur. This crucial problem is avoided in a toroidal geometry as illustrated in Fig. 8.4(b). Here, particles again spiral continuously along field lines. However, they never make contact with the first wall since the field lines do not leave the chamber in a toroidal geometry and the particle's perpendicular excursions are very small: $r_{Li} \ll a$.

It should be noted that various ingenious configurations have been invented to “plug” the ends of open ended systems. These configurations are based on the “mirror” effect, which is discussed shortly. Even so, in practice, the end losses are just too great to overcome and it is for this reason that all the leading magnetic geometries for fusion applications are toroidal.

To reiterate, the gyro motion of charged particles in a static, homogeneous magnetic field serves as the basic building block for magnetic confinement of fusion plasma.

8.4 Motion in constant \mathbf{B} and \mathbf{E} fields: the $\mathbf{E} \times \mathbf{B}$ drift

The first additional contribution to the static magnetic field to consider corresponds to a constant (in space and time) electric field. This may seem a little strange in view of the discussion in Chapter 7, which demonstrates the highly effective ability of a plasma to shield electric fields. The compatibility of Debye shielding with the existence of electric fields is discussed as the analysis proceeds, and in fact it is shown that no contradictions arise.

For the moment, in keeping with the spirit of “single-particle motion”, it is simply assumed that constant electric and magnetic fields are prescribed. The challenge then is to determine the motion of a charged particle in the combined set of fields. The modifications to the original gyro motion separate into two contributions, one due to the parallel electric field and the other due to the perpendicular component. It is shown that the parallel component leads to a constant acceleration and the perpendicular component leads to an initially surprising drift perpendicular to both \mathbf{E} and \mathbf{B} known as the $\mathbf{E} \times \mathbf{B}$ drift.

8.4.1 Effect of a parallel electric field

In addition to the constant magnetic field $\mathbf{B} = B \mathbf{e}_z$, assume a constant electric field $\mathbf{E} = \mathbf{E}_\perp + E_\parallel \mathbf{e}_z$ exists in the plasma. Consider first the effect of the parallel electric field. The parallel component of Newton’s law reduces to

$$m \frac{dv_z}{dt} = q E_\parallel \quad v_z(0) = v_\parallel. \quad (8.21)$$

The solution is easily found and is given by

$$v_z(t) = v_\parallel + \frac{q}{m} E_\parallel t. \quad (8.22)$$

In addition to the free streaming motion associated with v_\parallel there is a constant acceleration due to the parallel electric field. Hypothetically the particle velocity would continue to increase monotonically and indefinitely until it became relativistic.

In practice, there is a reason why this does not often occur. The ability of electrons and ions to free stream along the magnetic field implies that the parallel electric field that can be generated in a plasma is in general very small, in accordance with the principles of Debye shielding. The actual parallel electric field is not, however, quite as small as predicted by Debye shielding because of the presence of Coulomb collisions. These collisions produce a small frictional drag on the parallel motion leading to a small, but finite plasma resistivity. This resistivity generates a small (but still higher than the Debye value), parallel electric field, similar to the small, but finite, voltage drop across a length of copper wire. The combination of a small electric field and the frictional drag force limits the maximum velocity achievable by a charged particle to non-relativistic values. The frictional drag force due to collisions is discussed in detail in the next chapter.

A final interesting point concerning parallel motion is that under certain conditions, the frictional drag due to collisions is too weak to prevent the slowing down of a certain

class of electrons in the plasma. In this situation the electrons do indeed accelerate to relativistic velocities. These electrons are appropriately called “runaway electrons” and this phenomenon is also discussed in the next chapter.

8.4.2 Effect of a perpendicular electric field

The next topic concerns the effect of a perpendicular electric field on gyro motion. Consider first the mathematical solution to the problem. To simplify the analysis assume that $\mathbf{E}_\perp = E_x \mathbf{e}_x$, where $E_x = \text{const}$. The perpendicular equations of motion become

$$\begin{aligned} \frac{dv_x}{dt} &= \omega_c v_y + \frac{q}{m} E_x, \\ \frac{dv_y}{dt} &= -\omega_c v_x. \end{aligned} \quad (8.23)$$

Eliminating v_x by means of the second equation yields

$$\frac{d^2 v_y}{dt^2} + \omega_c^2 \left(v_y + \frac{E_x}{B} \right) = 0. \quad (8.24)$$

The solution is easily found by introducing a new velocity variable $v'_y = v_y + E_x/B$. The equation for v'_y simplifies to

$$\frac{d^2 v'_y}{dt^2} + \omega_c^2 v'_y = 0 \quad (8.25)$$

and corresponds to the gyro motion previously discussed.

The solution for the original velocity thus becomes

$$\mathbf{v}_\perp(t) = \mathbf{v}_{\text{gyro}}(t) - (E_x/B)\mathbf{e}_y. \quad (8.26)$$

Note the addition of a new drift perpendicular to both \mathbf{E} and \mathbf{B} . This result is easily generalized to an arbitrary perpendicular electric field $\mathbf{E}_\perp = E_x \mathbf{e}_x + E_y \mathbf{e}_y$, where E_x, E_y are constants. For the general case one introduces a new perpendicular velocity variable

$$\mathbf{v}'_\perp = \mathbf{v}_\perp - \mathbf{E}_\perp \times \mathbf{B}/B^2. \quad (8.27)$$

The basic equation of motion for the perpendicular (x, y) components, given by

$$m \frac{d\mathbf{v}_\perp}{dt} = q(\mathbf{E}_\perp + \mathbf{v}_\perp \times \mathbf{B}), \quad (8.28)$$

reduces to

$$\frac{d\mathbf{v}'_\perp}{dt} = \omega_c \mathbf{v}'_\perp \times \mathbf{e}_z. \quad (8.29)$$

Equation (8.29) corresponds to gyro motion in a uniform magnetic field. The general form for the original velocity can, therefore, be written as

$$\begin{aligned} \mathbf{v}_\perp(t) &= \mathbf{v}_{\text{gyro}}(t) + \mathbf{V}_E, \\ \mathbf{V}_E &= \frac{\mathbf{E} \times \mathbf{B}}{B^2}. \end{aligned} \quad (8.30)$$

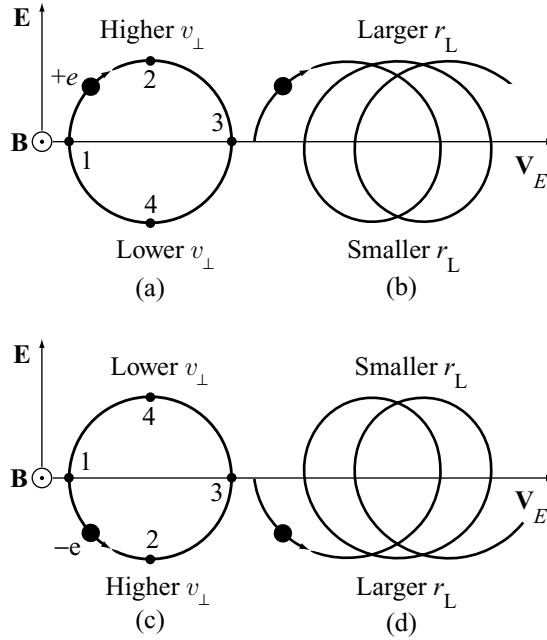


Figure 8.5 (a) Effect of \mathbf{E}_\perp on a positive charge and (b) the resulting perpendicular $\mathbf{E} \times \mathbf{B}$ drift. (c) Effect of \mathbf{E}_\perp on a negative charge and (d) the resulting perpendicular $\mathbf{E} \times \mathbf{B}$ drift.

The conclusion is that the addition of a uniform perpendicular electric field superimposes a constant drift velocity (\mathbf{V}_E) on the gyro motion. This drift is known as the $\mathbf{E} \times \mathbf{B}$ drift and is perpendicular to both \mathbf{E} and \mathbf{B} . It is also independent of the mass and charge. In other words, electrons and ions drift with the same velocity.

The next step is to develop a physical picture of the origin of the $\mathbf{E} \times \mathbf{B}$ drift and then lastly to address the issue of how the existence of a perpendicular electric field can be compatible with Debye shielding. A physical picture of the $\mathbf{E} \times \mathbf{B}$ drift can be obtained by examining Fig. 8.5 and recalling that the gyro radius increases with the perpendicular velocity: $r_L \sim v_\perp/B$. Consider the motion of a positive charge located in an electric and magnetic field as shown in Fig. 8.5(a). This illustration shows the gyro motion of the charge *without* the electric field. As the particle moves from point 1 to point 2, the effect of the electric field, because of its direction, is to accelerate the charge – increase its velocity. As it moves from point 2 to point 3 it slows down returning to its original velocity. Note that at every point along the top part of the trajectory the velocity is larger than the original velocity without the electric field, implying that on average its gyro radius has increased in size.

The opposite is true on the lower portion of the curve. From point 3 to point 4 the charge is decelerated and slows down. From point 4 back to point 1 the charge accelerates back to its original velocity. Over the bottom portion of the trajectory the average velocity and therefore the average gyro radius is smaller than without the electric field.

The combination of these effects is shown in Fig. 8.5(b). A higher v_{\perp} on the top portion of the trajectory and a lower v_{\perp} on the bottom portion lead to a drift perpendicular to both \mathbf{E} and \mathbf{B} resulting from the different sizes of the average gyro radius. A similar picture holds for negatively charged electrons as shown in Figs. 8.5(c) and 8.5(d). Observe that the direction of the drift is independent of the size of the charge.

Lastly the simultaneous existence of a perpendicular electric field and Debye shielding has to be reconciled. There are two points to consider. First note that since both electrons and ions have the same $\mathbf{E} \times \mathbf{B}$ drift velocity this corresponds to a macroscopic fluid flow $\mathbf{u}_{\perp} = \mathbf{V}_E$ without the generation of any electric current $\mathbf{J}_{\perp} = en(\mathbf{u}_{\perp i} - \mathbf{u}_{\perp e}) = 0$. The expression for the $\mathbf{E} \times \mathbf{B}$ drift velocity can thus be rewritten as $\mathbf{E}_{\perp} + \mathbf{u}_{\perp} \times \mathbf{B} = 0$. Now recall from the theory of low-frequency electromagnetism that the electric and magnetic fields in a fluid moving with a velocity \mathbf{u}_{\perp} can be transformed to the reference frame moving with the fluid by the relations $\mathbf{E}'_{\perp} = \mathbf{E}_{\perp} + \mathbf{u}_{\perp} \times \mathbf{B}$ and $\mathbf{B}' = \mathbf{B}$. Consequently, in the reference frame where the fluid is stationary it follows that $\mathbf{E}'_{\perp} = 0$, which is consistent with the principles of Debye shielding.

The second point is slightly more subtle. In future chapters it will be shown that small perpendicular electric fields (but still larger than the predicted Debye value) can exist in a plasma. This involves the development and solution of self-consistent plasma models. Qualitatively, such electric fields arise because perpendicular to \mathbf{B} the electrons and ions are magnetically confined and therefore are not free to flow and shield out any local charge imbalances that may develop. It will be shown that these imbalances are a consequence of the different size electron and ion gyro radii and ultimately lead to potentials on the order of $e\phi \sim T$.

In summary, the $\mathbf{E} \times \mathbf{B}$ drift is one of the fundamental cross-field drift velocities appearing in the guiding center theory of charged particle motion.

8.5 Motion in fields with perpendicular gradients: the ∇B drift

The second modification to gyro motion to be investigated involves inhomogeneities in the fields. Specifically, this section includes the effects of gradients in \mathbf{B} and \mathbf{E} perpendicular to the magnetic field. Although the \mathbf{B} field is inhomogeneous, its direction nevertheless remains straight; that is, \mathbf{B} is assumed to be of the form $\mathbf{B} = B(x, y)\mathbf{e}_z$. For the electric field, the gradients allowed are given by $\mathbf{E} = E_x(x)\mathbf{e}_x + E_y(y)\mathbf{e}_y$. Note that $\nabla \times \mathbf{E} = 0$. Were this not the case, then from Faraday's law, a time dependence would have to be included in \mathbf{B} . The time dependence issues are discussed in Section 8.7. The form of field gradients considered here appear in plasmas created in long, straight, solenoidal coils.

The analysis presented below demonstrates that the magnetic field gradient produces a particle drift perpendicular to both \mathbf{B} and ∇B known as the ∇B drift. The gradient in the electric field is shown to produce a small shift in the gyro frequency, which is of no great consequence for present purposes. The analysis is carried out using a straightforward perturbation expansion. The small parameter in the expansion is the ratio of the gyro radius to the

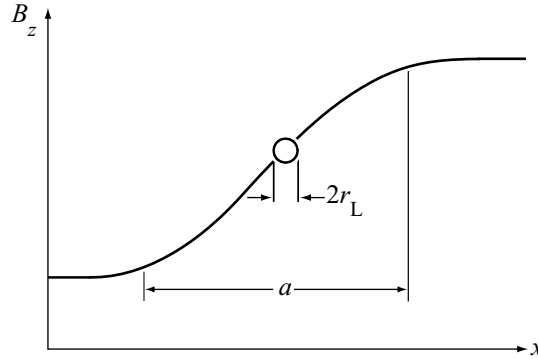


Figure 8.6 Width of the x dimension of a gyro orbit in a field with a weak gradient: $r_L \ll a$.

scale length characterizing the field inhomogeneities: $r_L \nabla B/B \sim r_L \nabla E/E \sim r_L/a \ll 1$. The magnetic and electric fields vary slowly compared to the gyro radius. The details of the perturbation expansion proceed as follows.

8.5.1 Perpendicular gradient in B with $E = 0$

To simplify the calculation assume initially that $\mathbf{E} = 0$ and $B(x, y) \rightarrow B(x)$. These assumptions are relaxed shortly. The perpendicular equations of motion can then be written as

$$\begin{aligned} m dv_x/dt &= q B(x) v_y, \\ m dv_y/dt &= -q B(x) v_x, \\ dx/dt &= v_x, \\ dy/dt &= v_y. \end{aligned} \quad (8.31)$$

These equations are complicated non-linear differential equations because of the x dependence of B . The equations are simplified by exploiting the small gyro radius approximation. The key step is to Taylor expand B about its guiding center. The implication is that a weak field gradient only allows a particle's x position to deviate slightly from its guiding center trajectory. See Fig. 8.6. Under this assumption, the perpendicular equations of motion can be written as

$$\begin{aligned} dv_x/dt &\approx \omega_c(x_g) \left[1 + \frac{\partial B(x_g)}{\partial x_g} \frac{x - x_g}{B(x_g)} \right] v_y, \\ dv_y/dt &\approx -\omega_c(x_g) \left[1 + \frac{\partial B(x_g)}{\partial x_g} \frac{x - x_g}{B(x_g)} \right] v_x, \\ dx/dt &= v_x, \\ dy/dt &= v_y. \end{aligned} \quad (8.32)$$

Note that the magnitude of second term in the square bracket is smaller by the ratio r_L/a .

The solution to Eq. (8.32) is found by a straightforward perturbation expansion:

$$\begin{aligned} \mathbf{v} &= \mathbf{v}_0 + \mathbf{v}_1 + \cdots, \\ \mathbf{r} &= \mathbf{r}_0 + \mathbf{r}_1 + \cdots. \end{aligned} \quad (8.33)$$

The expansion is substituted into the equations of motion. Setting the leading order contribution to zero yields

$$\begin{aligned} d\mathbf{v}_0/dt &= \omega_c \mathbf{v}_0 \times \mathbf{e}_z, \\ d\mathbf{r}_0/dt &= \mathbf{v}_0. \end{aligned} \quad (8.34)$$

Since $\omega_c = \omega_c(x_g) = \text{const.}$, the solution to Eq. (8.34) is simply the basic gyro motion given by Eqs. (8.15) and (8.16).

The zero order solution is now substituted into the first order contribution to the perturbation equations, which can be written as

$$\begin{aligned} \frac{dv_{x1}}{dt} - \omega_c v_{y1} &= -\frac{v_\perp^2}{2B} \frac{\partial B}{\partial x_g} [1 - \cos 2(\omega_c t - \phi)], \\ \frac{dv_{y1}}{dt} - \omega_c v_{x1} &= -\frac{v_\perp^2}{2B} \frac{\partial B}{\partial x_g} \sin 2(\omega_c t - \phi). \end{aligned} \quad (8.35)$$

These are linear inhomogeneous differential equations. Observe that there are two types of driving terms – a constant term and a term oscillating at twice the gyro frequency. Since the equations are linear the response to each type of driving term can be determined by superposition. It is shown in Problem 8.2 that the second harmonic terms give rise to a small shift in the location of the guiding center plus a small correction to the size of the gyro radius. Neither of these effects is of any consequence since they do not result in a guiding center drift. They can thus be ignored for present purposes. Under this assumption the equations for the velocity components reduce to

$$\begin{aligned} \frac{dv_{x1}}{dt} - \omega_c v_{y1} &= -\frac{v_\perp^2}{2B} \frac{\partial B}{\partial x_g}, \\ \frac{dv_{y1}}{dt} + \omega_c v_{x1} &= 0. \end{aligned} \quad (8.36)$$

These equations are identical in form to Eq. (8.23), which produced the $\mathbf{E} \times \mathbf{B}$ drift. By direct comparison it follows that any driving term representing a constant acceleration $\mathbf{F}/m \rightarrow q \mathbf{E}/m$ gives rise to an equivalent $\mathbf{E} \times \mathbf{B}$ drift of the form

$$\mathbf{V}_F = \frac{1}{q} \frac{\mathbf{F} \times \mathbf{B}}{B^2}. \quad (8.37)$$

Applying this result to Eq. (8.26) leads to the ∇B drift

$$\mathbf{V}_{\nabla B} = \frac{v_\perp^2}{2\omega_c} \frac{1}{B} \frac{\partial B}{\partial x_g} \mathbf{e}_y. \quad (8.38)$$

In Problem 8.2 it is shown that this result can be easily generalized to the 2-D case $B = B(x, y)$. The result is a generalized form of the ∇B drift given by

$$\mathbf{V}_{\nabla B} = \mp \frac{v_\perp^2}{2\omega_c} \frac{\mathbf{B} \times \nabla B}{B^2}, \quad (8.39)$$

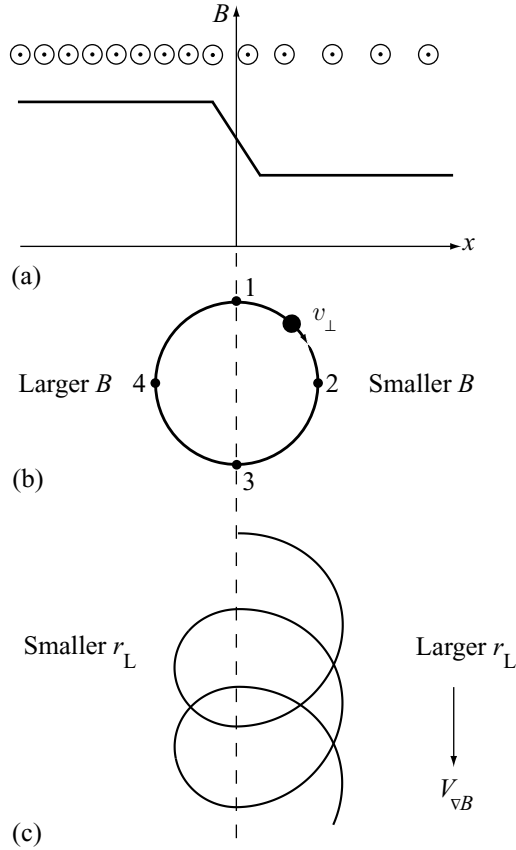


Figure 8.7 (a) Magnetic field gradient due to $\mathbf{B} = B(x)\mathbf{e}_z$. (b) Gyro motion ignoring the B field gradient. (c) Gyro motion plus the ∇B drift.

where the upper sign corresponds to a negative charge and it is understood that the field is evaluated at the guiding center.

Observe the following properties of the ∇B drift. (1) The drift is perpendicular to both \mathbf{B} and ∇B . (2) For a typical thermal particle ($v_{\perp} \sim v_T$) the ∇B drift is small compared to the thermal velocity: $|\mathbf{V}_{\nabla B}/v_T| \sim r_L/a$. (3) Since the drift is proportional to mv_{\perp}^2 it has the same (velocity-averaged) magnitude for electrons and ions when $T_e = T_i = T$. (4) Since $\mathbf{V}_{\nabla B}$ is proportional to $1/q$ the direction of the drift is opposite for electrons and ions, causing a net flow of current.

A physical picture of the ∇B drift can be obtained by examining Fig. 8.7. A magnetic field profile with an admittedly exaggerated magnetic field gradient is shown in Fig. 8.7(a) and Fig. 8.7(b) illustrates the zeroth order gyro motion for a positive particle in which the effects of the gradient are ignored. Recalling that the gyro radius scales as $r_L \sim v_{\perp}/B$, it follows that along the trajectory from point 1 to point 2 to point 3 the gyro radius will be

slightly larger because the magnetic field is slightly smaller. Similarly, from point 3 to point 4 and back to point 1 the gyro radius is slightly smaller because of the increased magnetic field. These modifications to gyro motion are combined in Fig. 8.7(c) demonstrating the existence of the ∇B drift. A similar picture holds for negative charges.

The ∇B drift makes an important contribution to the flow of current and the corresponding self-consistent magnetic field in a fusion plasma.

8.5.2 Perpendicular gradient in E with uniform B

The next topic involves the effects of a weak perpendicular gradient in the electric field. The magnetic field can be considered to be uniform ($B = \text{const.}$) since the effects of a weak gradient in B have already been calculated and, as has been shown, can be easily included by means of superposition. The derivation below demonstrates that the main effect of the electric field gradient is to produce a small correction to the gyro frequency which is of no great significance.

The analysis is carried out assuming the following form for the electric field: $\mathbf{E} = E_x(x)\mathbf{e}_x$. This form satisfies $\nabla \times \mathbf{E} = 0$ so that no time dependence need be included in the magnetic field. As with the ∇B drift, the mathematical solution is obtained by a straightforward perturbation technique in which the electric field is expanded about the guiding center position of the particle. The relevant equations for the velocity components become

$$\begin{aligned} \frac{dv_x}{dt} - \omega_c \left[v_y + \frac{E_x(x_g)}{B} \right] &\approx \frac{q}{m} \frac{\partial E_x}{\partial x_g} (x - x_g), \\ \frac{dv_y}{dt} + \omega_c v_x &= 0. \end{aligned} \quad (8.40)$$

Note, that if there were no gradient in the electric field the solution would be given by the sum of the gyro motion plus $\mathbf{E} \times \mathbf{B}$ drift as expected. When the gradient is included one must be careful before simply substituting the zeroth order solutions into the correction term on the right hand side of Eq. (8.40). The reason is that this term might oscillate at the fundamental gyro frequency, thereby appearing as a potentially resonant driving term in the equation. As is well known, a resonant driving term often leads to solutions that grow linearly with time. In other words, the solutions become linearly divergent with t and the perturbation procedure breaks down.

A more careful examination of Eq. (8.40) shows, however, that resonant growth does not occur and the solutions remain bounded. To see this, differentiate the first equation and then eliminate dv_y/dt by means of the second equation. A short calculation yields

$$\frac{d^2 v_x}{dt^2} + \omega_c^2 \left(1 - \frac{1}{\omega_c B} \frac{\partial E_x}{\partial x_g} \right) v_x = 0. \quad (8.41)$$

Equation (8.41) shows that the main effect of a perpendicular gradient in the electric field is to generate a small correction to the gyro frequency. There is no new particle drift or resonance. In other words, the effect is of no great consequence and is ignored hereafter.

Finally, it is worth noting that if one carries out the expansion one order higher in the ratio r_L/a a drift does develop known as the “finite gyro radius” drift. This drift is in the same direction for electrons and ions but is larger in magnitude for the ions. However, because of its small magnitude (r_L/a smaller than the other guiding center drifts) it does not play an important role for much of the fusion plasma physics discussed in this book. For this reason it is ignored hereafter, although it is discussed in Problem 8.3.

8.6 Motion in a curved magnetic field: the curvature drift

The spatial dependence of the magnetic fields thus far considered has been either uniform or possessing a perpendicular gradient. In all cases, however, the direction of the field has been straight, along the \mathbf{e}_z direction. The present section relaxes this constraint and allows for a curved magnetic field. It is shown that the field line curvature leads to a new guiding center drift perpendicular to both the magnetic field and the curvature vector. The drift is driven by the centrifugal force felt by a particle due to its free streaming, parallel motion along a curved field line. Hence, it is known as the “curvature drift.”

The analysis is first carried out for a simple curvilinear geometry in which the fields are assumed to be of the form $\mathbf{B} = B(r)\mathbf{e}_\theta$ and $\mathbf{E} = E_r(r)\mathbf{e}_r$. A perturbation expansion is again used. Once the drift has been calculated, the derivation is extended to a generalized curvilinear geometry. The first derivation begins by noting that in a cylindrical coordinate system the position, velocity, and acceleration are related by

$$\begin{aligned} \mathbf{r}(t) &= r(t)\mathbf{e}_r + z(t)\mathbf{e}_z, \\ \mathbf{v}(t) &= \frac{d\mathbf{r}}{dt} = \frac{dr}{dt}\mathbf{e}_r + r\frac{d\theta}{dt}\mathbf{e}_\theta + \frac{dz}{dt}\mathbf{e}_z = v_r\mathbf{e}_r + v_\theta\mathbf{e}_\theta + v_z\mathbf{e}_z, \\ \mathbf{a}(t) &= \frac{d\mathbf{v}}{dt} = \left(\frac{dv_r}{dt} - \frac{v_\theta^2}{r}\right)\mathbf{e}_r + \left(\frac{dv_\theta}{dt} + \frac{v_r v_\theta}{r}\right)\mathbf{e}_\theta + \frac{dv_z}{dt}\mathbf{e}_z. \end{aligned} \quad (8.42)$$

Here, use has been made of the fact that the directions of two of the unit vectors change with θ :

$$\begin{aligned} \frac{d\mathbf{e}_r}{dt} &= \frac{\partial \mathbf{e}_r}{\partial \theta} \frac{d\theta}{dt} = \frac{v_\theta}{r}\mathbf{e}_\theta, \\ \frac{d\mathbf{e}_\theta}{dt} &= \frac{\partial \mathbf{e}_\theta}{\partial \theta} \frac{d\theta}{dt} = -\frac{v_\theta}{r}\mathbf{e}_r. \end{aligned} \quad (8.43)$$

The equations of motion for the velocity components can now be written as

$$\begin{aligned} \frac{dv_r}{dt} - \frac{v_\theta^2}{r} &= \frac{q}{m}(E_r - v_z B), \\ \frac{dv_z}{dt} &= \frac{q}{m}v_r B, \\ \frac{dv_\theta}{dt} + \frac{v_r v_\theta}{r} &= 0. \end{aligned} \quad (8.44)$$

The dominant behavior again corresponds to gyro motion plus an $\mathbf{E} \times \mathbf{B}$ drift. This can be seen by introducing a perturbation expansion similar to the ∇B drift analysis: $\mathbf{v}(t) \approx \mathbf{v}_0(t) + \mathbf{v}_1(t)$. Here, $\mathbf{v}_0(t)$ consists of $\mathbf{v}_{\perp 0}(t) = \mathbf{v}_{\text{gyro}} + \mathbf{V}_E$ and $v_{\theta 0}(t) = v_{\parallel} = \text{const}$. Note that parallel now refers to the θ direction. The next step is to substitute into Eq. (8.44) and to expand all quantities about the guiding center position r_g . A short calculation yields an equation for $\mathbf{v}_1(t)$:

$$\begin{aligned} \frac{d\mathbf{v}_{\perp 1}}{dt} - \omega_c \mathbf{v}_{\perp 1} \times \mathbf{e}_{\theta} &= \frac{\omega_c(r - r_g)}{B} \left[\frac{\partial B}{\partial r_g} \mathbf{v}_{\perp 0} \times \mathbf{e}_{\theta} + \frac{\partial E_r}{\partial r_g} \mathbf{e}_r \right] + \frac{v_{\parallel}^2}{r_g} \mathbf{e}_r, \\ \frac{dv_{\parallel 1}}{dt} &= -\frac{v_{r0}v_{z0}}{r_g}, \end{aligned} \quad (8.45)$$

where $\omega_c = qB(r_g)/m$.

The solution has the following properties. The parallel velocity $v_{\parallel 1}(t)$ develops a small, unimportant, second harmonic modulation, a consequence of the fact that both $v_{r0}(t)$ and $v_{z0}(t)$ are oscillatory at the fundamental frequency and are $\pi/2$ out of phase. The first two terms on the right hand side of the $\mathbf{v}_{\perp 1}$ equation represent the ∇B drift and the $\mathbf{E}_{\perp}(\mathbf{r}_{\perp})$ gyro frequency correction already discussed. Only the last term represents a new contribution. Because the perturbation expansion essentially linearizes the first order equations, the effect of the new term can again be calculated using superposition.

Physically, this term represents the centrifugal force acting on the particle because of its free streaming parallel motion along a curved magnetic field line. Mathematically, the term has the form of a constant external force. Therefore, in accordance with Eq. (8.37) a guiding center drift develops that is perpendicular to both the magnetic field and the centrifugal force. It is known as the curvature drift and is given by

$$\mathbf{V}_{\kappa} = \frac{v_{\parallel}^2}{\omega_c r} \mathbf{e}_z \quad (8.46)$$

with all quantities evaluated at the guiding center. The drift has a similar scaling as $\mathbf{V}_{\nabla B}$ except that v_{\perp}^2 is replaced with $2v_{\parallel}^2$. It is small compared to the thermal velocity ($|\mathbf{V}_{\kappa}|/v_T \sim r_L/a$) and comparable in magnitude for electrons and ions of similar temperatures. The direction of the curvature drift for electrons is opposite to that for ions and therefore generates a current.

The expression for \mathbf{V}_{κ} can be generalized to an arbitrary curvilinear magnetic geometry by introducing the radius of curvature vector \mathbf{R}_c . Several steps are required. First, the unit vector parallel to the magnetic field is introduced: $\mathbf{b}(\mathbf{r}) \equiv \mathbf{B}/B$. Second, the velocity vector is decomposed into a perpendicular and a parallel component: $\mathbf{v}(t) = \mathbf{v}_{\perp} + v_{\parallel} \mathbf{b}$. Next, the perpendicular components of the equations of motion (with $\mathbf{E} = 0$ for simplicity) are extracted by forming the operation

$$\mathbf{b} \times \left\{ \left[\frac{d}{dt} (\mathbf{v}_{\perp} + v_{\parallel} \mathbf{b}) - \omega_c (\mathbf{v}_{\perp} + v_{\parallel} \mathbf{b}) \times \mathbf{b} \right] \times \mathbf{b} \right\} = 0, \quad (8.47)$$

where $\omega_c = qB(\mathbf{r})/m$. The various terms are simplified as follows:

$$\begin{aligned} \mathbf{b} \times \{[\omega_c(\mathbf{v}_\perp + v_\parallel \mathbf{b}) \times \mathbf{b}] \times \mathbf{b}\} &= -\omega_c \mathbf{v}_\perp \times \mathbf{b}, \\ \mathbf{b} \times \left\{ \left[\frac{d\mathbf{v}_\perp}{dt} \right] \times \mathbf{b} \right\} &= \left(\frac{d\mathbf{v}_\perp}{dt} \right)_\perp, \\ \mathbf{b} \times \left\{ \left[\frac{d}{dt}(v_\parallel \mathbf{b}) \right] \times \mathbf{b} \right\} &= v_\parallel \mathbf{b} \times \left[\left(\frac{d\mathbf{b}}{dt} \right) \times \mathbf{b} \right] \\ &= v_\parallel \left[(\mathbf{b} \cdot \mathbf{b}) \frac{d\mathbf{b}}{dt} - \left(\mathbf{b} \cdot \frac{d\mathbf{b}}{dt} \right) \mathbf{b} \right]. \end{aligned} \quad (8.48)$$

The last term can be further simplified by noting that for a unit vector $\mathbf{b} \cdot \mathbf{b} = 1$ and therefore $\mathbf{b} \cdot d\mathbf{b}/dt = (1/2)d(\mathbf{b} \cdot \mathbf{b})/dt = 0$. Also, the term $d\mathbf{b}/dt$ can be rewritten as

$$\frac{d\mathbf{b}(\mathbf{r})}{dt} = \left(\frac{\partial}{\partial t} + \frac{d\mathbf{r}}{dt} \cdot \nabla \right) \mathbf{b} = \mathbf{v} \cdot \nabla \mathbf{b}. \quad (8.49)$$

Combining results leads to a simpler form of the perpendicular equations of motion:

$$\left(\frac{d\mathbf{v}_\perp}{dt} \right)_\perp - \omega_c \mathbf{v}_\perp \times \mathbf{b} = -v_\parallel \mathbf{v}_\perp \cdot \nabla \mathbf{b} - v_\parallel^2 \mathbf{b} \cdot \nabla \mathbf{b}. \quad (8.50)$$

The left hand side of this equation represents the familiar gyro motion. In the context of a perturbation expansion the right hand side of the equation represents two inhomogeneous driving terms, both smaller by r_\perp/a . The term with $v_\parallel \mathbf{v}_\perp$ oscillates at the gyro frequency with zero average value. It thus makes small modifications to the gyro motion as previously discussed, but does not lead to a drift of the guiding center. Only the last term has the form of a constant external force. It represents the generalization of the centrifugal force and leads to the curvature drift.

The last step in the analysis is to determine a relation between the magnetic curvature vector $\mathbf{b} \cdot \nabla \mathbf{b}$ and the radius of curvature vector \mathbf{R}_c . This relationship is easily established by examining Fig. 8.8. Observe that the change in \mathbf{b} along a curved magnetic line is given by

$$\begin{aligned} d\mathbf{b} &= \mathbf{b}(\mathbf{r}_\perp, l + dl) - \mathbf{b}(\mathbf{r}_\perp, l) = \frac{\partial \mathbf{b}}{\partial l} dl = (\mathbf{b} \cdot \nabla \mathbf{b}) dl, \\ |d\mathbf{b}| &= d\theta = \frac{dl}{R_c}. \end{aligned} \quad (8.51)$$

Here use has been made of the fact that the change along the magnetic field is equivalent to taking the parallel gradient: $\partial/\partial l = \mathbf{b} \cdot \nabla$. From the geometry and the definition of the radius of curvature vector it is clear that \mathbf{R}_c is anti-parallel to $\mathbf{b} \cdot \nabla \mathbf{b}$. Therefore $\mathbf{R}_c = -K \mathbf{b} \cdot \nabla \mathbf{b}$. The scale factor K is found by noting that $|\mathbf{b} \cdot \nabla \mathbf{b}| = |d\mathbf{b}|/dl = 1/R_c$. Combining results

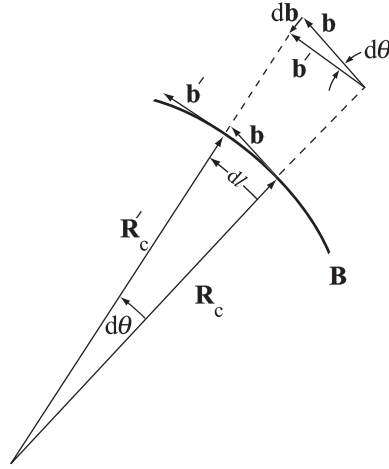


Figure 8.8 Geometry showing the relation between $\mathbf{b} \cdot \nabla \mathbf{b}$ and \mathbf{R}_c . Here, $\mathbf{b} = \mathbf{b}(\mathbf{r}_{\perp}, l)$ and $\mathbf{b}' = \mathbf{b}(\mathbf{r}_{\perp}, l + dl)$. Similarly for \mathbf{R}_c and \mathbf{R}'_c .

leads to

$$\mathbf{b} \cdot \nabla \mathbf{b} = -\frac{\mathbf{R}_c}{R_c^2}. \tag{8.52}$$

The generalized form of the curvature drift can now be calculated. Equation (8.52) is substituted into the centrifugal force term in Eq. (8.50). Then, using the relation between a constant external force and the resulting guiding center drift given by Eq. (8.37), one obtains the desired generalization:

$$\mathbf{V}_{\kappa} = \mp \frac{v_{\parallel}^2}{\omega_c} \frac{\mathbf{R}_c \times \mathbf{B}}{R_c^2 B}. \tag{8.53}$$

Again the top sign refers to electrons.

Like the ∇B drift, the curvature drift makes an important contribution to the flow of current in a plasma and the determination of the self-consistent magnetic fields.

8.7 Combined $V_{\nabla B}$ and V_{κ} drifts in a vacuum magnetic field

In a steady state fusion plasma with $\mathbf{E} = 0$, an inhomogeneous, curved magnetic field produces two guiding center drifts – the ∇B drift and the curvature drift. For the special situation where the plasma currents are small, the magnetic field becomes approximately a vacuum magnetic field and a simplifying relationship exists between $V_{\nabla B}$ and V_{κ} . The goal of this section is to derive this relationship. It is shown that for vacuum fields $V_{\nabla B}$ and V_{κ} are both in the same direction, implying that there is no way for their resulting currents to cancel.

The derivation follows from the well-known vector identity

$$\nabla(\mathbf{B} \cdot \mathbf{B}) = 2\mathbf{B} \times (\nabla \times \mathbf{B}) + 2\mathbf{B} \cdot \nabla \mathbf{B}. \quad (8.54)$$

For a vacuum magnetic field $\nabla \times \mathbf{B} = 0$. One now forms the cross product of Eq. (8.54) with \mathbf{b} . A short calculation yields

$$\mathbf{B} \times \nabla B = B \mathbf{b} \times [\mathbf{b}(\mathbf{b} \cdot \nabla B) + B \mathbf{b} \cdot \nabla \mathbf{b}] = -B \frac{\mathbf{B} \times \mathbf{R}_c}{R_c^2}. \quad (8.55)$$

Using this relation in the expression for the ∇B drift (Eq. (8.39)) leads to a simple expression for $\mathbf{V}_{\nabla B} + \mathbf{V}_\kappa$:

$$\mathbf{V}_\kappa + \mathbf{V}_{\nabla B} = \mp \frac{1}{\omega_c} (v_\parallel^2 + \frac{v_\perp^2}{2}) \frac{\mathbf{R}_c \times \mathbf{B}}{R_c^2 B}. \quad (8.56)$$

As stated, each drift is obviously in the same direction and hence the resulting currents cannot cancel. This leads to the following interesting question. If the guiding center currents always add, and if $\mathbf{V}_{\nabla B}$ and \mathbf{V}_κ are the only current-producing guiding center drifts associated with an inhomogeneous, curved magnetic field, how then can \mathbf{B} correspond to a vacuum field? The answer lies in the development of an additional macroscopic fluid like current, known as the “magnetization current”, which exactly cancels the $\mathbf{V}_{\nabla B} + \mathbf{V}_\kappa$ contribution to \mathbf{J} . A discussion of the magnetization current is deferred until Chapter 10, where self-consistent fluid models are developed.

8.8 Motion in time varying \mathbf{E} and \mathbf{B} fields: the polarization drift

The next contribution to the theory of single-particle guiding center motion involves the effects of slow time varying electric and magnetic fields. Specifically, attention is focused on fields of the form $\mathbf{E}(\mathbf{r}, t) = E_x(\mathbf{r}_\perp, t)\mathbf{e}_x + E_y(\mathbf{r}_\perp, t)\mathbf{e}_y$ and $\mathbf{B} = B(\mathbf{r}_\perp, t)\mathbf{e}_z$. It is shown that the main consequences of the time variation are the development of a new guiding center drift known as the “polarization drift” and the identification of a new approximate constant of the motion known as the “adiabatic invariant.”

The polarization drift arises from the effects of particle inertia in a time varying electric field. As \mathbf{E}_\perp changes slowly in time the particle motion tracks the time evolution of the field, although lagging slightly behind because of particle inertia. The analysis demonstrates that the resulting polarization drift is in the direction of \mathbf{E}_\perp (and not $\mathbf{E}_\perp \times \mathbf{B}$) and is larger for ions than electrons because of the heavier ion mass.

The adiabatic invariant predicts how the perpendicular energy of a charged particle evolves in time in the presence of a slowly varying magnetic field. It is shown that an increasing \mathbf{B} field causes a corresponding increase in v_\perp^2 . The invariant is not an exact constant of the motion in the sense that its value remains unchanged only after time averaging over the gyro motion.

The analysis is separated into two parts. In the first part the magnetic field is assumed to be uniform in space and time ($B = \text{const.}$) and the electric field is assumed to vary only with time ($\mathbf{E} = E_x(t)\mathbf{e}_x + E_y(t)\mathbf{e}_y$). This simplified model captures the essential features of the polarization drift. The mathematical solution is obtained by a straightforward iteration procedure.

The second part of the analysis allows the magnetic field to also be a function of time. This slightly complicates the calculation because a time varying \mathbf{B} field generates a spatially varying electric field in accordance with Faraday's law. These effects are treated by introducing a special mathematical time transformation into the analysis. Two results follow. First, there is a slight modification to the polarization drift. Second, the new approximate constant of the motion is derived. This constant is known as the adiabatic invariant μ .

8.8.1 The polarization drift for $E_\perp = E_x(t)\mathbf{e}_x + E_y(t)\mathbf{e}_y$ and $B = \text{const.}$

This subsection focuses on the simple form of the fields given above. The mathematical analysis of the polarization drift is presented first, followed by a simple physical picture.

Mathematical derivation

For the fields under consideration the equations of motion for the perpendicular particle velocity are given by

$$\begin{aligned} dv_x/dt - \omega_c v_y &= \omega_c E_x(t)/B, \\ dv_y/dt + \omega_c v_x &= \omega_c E_y(t)/B. \end{aligned} \quad (8.57)$$

A formal exact mathematical solution to these equations is readily obtainable for arbitrary E_x, E_y . However, the solutions are not very insightful since they involve a variety of complicated integrals. Insight can ultimately be obtained by making use of the slow time variation assumption, which then allows an approximate evaluation of the integrals.

For present purposes, it is more convenient mathematically to assume slow variation from the outset. With this assumption, one can obtain an accurate approximation to the solution by means of a straightforward iteration procedure. The basis for the procedure is the introduction of a small parameter that measures the slowness of the time variation. Specifically, the characteristic frequency ω associated with the time variation of the electric fields is assumed to be low compared to the gyro frequency: $|\dot{\mathbf{E}}_\perp|/|\mathbf{E}_\perp| \sim \omega \ll \omega_c$. The low-frequency assumption guarantees that each new term in the iteration is smaller by ω/ω_c than the previous term.

The first step in the iteration procedure is to introduce a new velocity variable \mathbf{v}'_\perp that subtracts out the $\mathbf{E} \times \mathbf{B}$ drift.

$$\begin{aligned} v_x &= v'_x + E_y(t)/B, \\ v_y &= v'_y - E_x(t)/B. \end{aligned} \quad (8.58)$$

The equations of motion for \mathbf{v}'_{\perp} become

$$\begin{aligned}\frac{dv'_x}{dt} - \omega_c v'_y &= -\frac{1}{B} \frac{dE_y}{dt}, \\ \frac{dv'_y}{dt} + \omega_c v'_x &= \frac{1}{B} \frac{dE_x}{dt}.\end{aligned}\tag{8.59}$$

Note that the right hand side of Eq. (8.59) is smaller by ω/ω_c than the corresponding terms in Eq. (8.57).

The next step in the iteration is to treat the terms on the right hand side of Eq. (8.59) as a new “constant” (actually slowly varying) external force. In analogy with the $\mathbf{E} \times \mathbf{B}$ drift, these terms can be explicitly separated out from the solution by introducing a new velocity variable \mathbf{v}''_{\perp} as follows:

$$\begin{aligned}v'_x &= v''_x + \frac{1}{\omega_c B} \frac{dE_x}{dt}, \\ v'_y &= v''_y + \frac{1}{\omega_c B} \frac{dE_y}{dt}.\end{aligned}\tag{8.60}$$

The equations for \mathbf{v}''_{\perp} are now given by

$$\begin{aligned}\frac{dv''_x}{dt} - \omega_c v''_y &= -\frac{1}{\omega_c B} \frac{d^2 E_x}{dt^2} \approx 0, \\ \frac{dv''_y}{dt} + \omega_c v''_x &= -\frac{1}{\omega_c B} \frac{d^2 E_y}{dt^2} \approx 0.\end{aligned}\tag{8.61}$$

The terms on the right hand side of Eq. (8.61) can be neglected since they involve the same components of electric field as the starting equations and are smaller by $(\omega/\omega_c)^2$. In principle, one could continue with the iteration procedure to higher and higher order, although it is obvious by construction that each new right hand side driving term is smaller by ω/ω_c than the previous iteration. Once the higher order terms in Eq. (8.61) are neglected it is clear that the solution for \mathbf{v}''_{\perp} is just the familiar gyro motion.

The conclusion from the analysis is that in a constant B field with a slowly varying perpendicular electric field the combined orbit of the particle is accurately approximated by

$$\mathbf{v}_{\perp}(t) = \mathbf{v}_{\text{gyro}} + \frac{\mathbf{E}_{\perp} \times \mathbf{B}}{B^2} + \mathbf{V}_p,\tag{8.62}$$

where (with the upper sign corresponding to electrons)

$$\mathbf{V}_p = \mp \frac{1}{\omega_c B} \frac{d\mathbf{E}_{\perp}}{dt}.\tag{8.63}$$

Observe the following properties of the solution. The velocity consists mainly of gyro motion plus the instantaneous value of the $\mathbf{E} \times \mathbf{B}$ drift. This is what one might expect from a slowly varying electric field. There is, however, a small additional drift velocity \mathbf{V}_p in the direction of the electric field and this is the polarization drift. It flows in opposite direction for electrons and ions (tending to cause a charge “polarization” in the direction

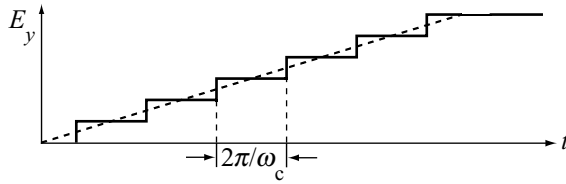


Figure 8.9 Dashed curve: linearly rising electric field that levels off after a period of time. Solid curve: step function model of the electric field evolution.

of the electric field) and is much larger for ions because of their heavier mass. In terms of its magnitude, the polarization drift is small compared to the $\mathbf{E} \times \mathbf{B}$ drift. In particular, $\mathbf{V}_p/\mathbf{V}_E \sim \omega/\omega_c \ll 1$. One might ask if \mathbf{V}_p is small why keep it at all? The reason is that while it is small, it is still the first non-zero perpendicular drift in the direction of \mathbf{E}_\perp . There is clearly no contribution in this direction from the $\mathbf{E} \times \mathbf{B}$ drift.

The difference in direction is important. In terms of currents flowing in the direction of \mathbf{E}_\perp it makes more sense to compare the polarization drift with the displacement current which also points in the same direction. This comparison is easily made by calculating

$$\begin{aligned} \mathbf{J}_p &\approx qn\mathbf{V}_{pi} = \frac{nm_i}{B^2} \frac{d\mathbf{E}_\perp}{dt}, \\ \mathbf{J}_d &= \epsilon_0 \frac{\partial \mathbf{E}_\perp}{\partial t}. \end{aligned} \quad (8.64)$$

The ratio of polarization to displacement currents is thus given by

$$\frac{\mathbf{J}_p}{\mathbf{J}_d} = \frac{c^2}{v_A^2}, \quad (8.65)$$

where $v_A = (B^2/\mu_0 nm_i)^{1/2}$ is known as the Alfvén speed. For typical reactor parameters, this ratio is about $3 \times 10^3 \gg 1$. In the comparison, the polarization current is dominant.

A physical picture

The physical origin of the polarization drift is associated with the inertia of the particles. To understand how the drift arises consider the motion of a positively charged particle in a constant B field and a linearly time varying E_y as shown in Fig. 8.9. Now, for simplicity, approximate the time behavior of the electric field as a series of increasing steps with the duration of each step corresponding to one gyro period.

A qualitative picture of the orbit under the action of these fields is illustrated in Fig. 8.10. The dashed curve is a reference circular gyro orbit with no electric field. The solid curve is the orbit during the first step of the electric field. Note that in addition to the $\mathbf{E} \times \mathbf{B}$ shift of the guiding center to the right, both the top and bottom points of the trajectory (i.e., points 1 and 2), are shifted slightly upward because of the different average gyro radius size in the upper and lower portions of the orbit. This difference in gyro radius is associated with inertia which causes the particle motion to lag behind the changing electric field.

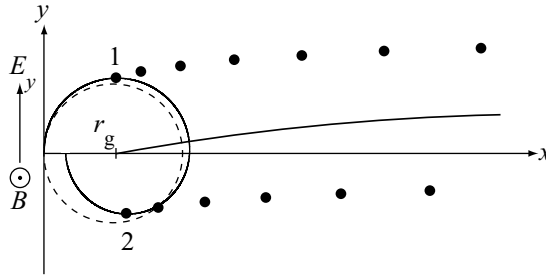


Figure 8.10 Locus of the maximum, minimum, and guiding center location of the particle orbit for the step model of the electric field.

During the second step the process repeats itself with the following modifications due to the larger value of the electric field. The $\mathbf{E} \times \mathbf{B}$ shift of the guiding center to the right is slightly larger. Similarly, the upward shifts of point 1 and point 2 are also both larger. Figure 8.10 plots the envelopes of point 1, point 2 and \mathbf{r}_g for consecutive steps in the electric field. There is clearly a drift of the guiding center in the y direction as long as the electric field is varying in time. This is the polarization drift. Once the electric field levels off the polarization drift vanishes and all that remains is a constant $\mathbf{E} \times \mathbf{B}$ drift.

8.8.2 The polarization drift for $\mathbf{E}_\perp = E_x(\mathbf{r}_\perp, t)\mathbf{e}_x + E_y(\mathbf{r}_\perp, t)\mathbf{e}_y$ and $\mathbf{B} = B(t)\mathbf{e}_z$

In this subsection the analysis of the polarization drift is generalized to include the effect of a time varying magnetic field. A further result is the identification of the adiabatic invariant μ as an approximate constant of the motion.

Note that for simplicity the perpendicular spatial dependence of B is ignored as these effects have already been investigated. Even so, a time varying magnetic field complicates the analysis by requiring a time and spatially varying electric field because of Faraday's law. These effects are treated by means of a mathematical transformation of the time variable which greatly simplifies the analysis.

Mathematical analysis

The calculation begins by assuming that the perpendicular electric field is of the form $\mathbf{E}_\perp = E_y(x, t)\mathbf{e}_y$, a simplification that helps to keep the algebra tractable but still captures the essential physics under consideration. With some straightforward additional work the calculation can be easily generalized to the case $\mathbf{E}_\perp = E_x(\mathbf{r}_\perp, t)\mathbf{e}_x + E_y(\mathbf{r}_\perp, t)\mathbf{e}_y$. The starting model corresponds to the equations of motion with the electric field expanded about the guiding center of the particle:

$$\begin{aligned} \frac{dv_x}{dt} - \omega_c v_y &= 0, \\ \frac{dv_y}{dt} + \omega_c v_x &= \frac{\omega_c}{B} \left[E_y + \frac{\partial E_y}{\partial x_g} (x - x_g) \right]. \end{aligned} \quad (8.66)$$

Here, $\omega_c(t) = qB(t)/m$ and all the electric field terms are functions of (x_g, t) . Note that even the pure gyro motion is difficult to calculate in the present form of the equations because of the time dependent gyro frequency. The equations are greatly simplified by introducing a new time variable τ defined by

$$\tau = \int_0^t \omega_c(t') dt', \quad (8.67)$$

implying that $d\tau = \omega_c dt$. Under this transformation the model reduces to

$$\begin{aligned} \frac{dv_x}{d\tau} - v_y &= 0, \\ \frac{dv_y}{d\tau} + v_x &= \frac{1}{B} \left[E_y + \frac{\partial E_y}{\partial x_g} (x - x_g) \right], \\ \frac{dx}{d\tau} &= \frac{v_x}{\omega_c}, \\ \frac{dy}{d\tau} &= \frac{v_y}{\omega_c}. \end{aligned} \quad (8.68)$$

An accurate approximate solution to these equations can be obtained by introducing the iteration procedure of the previous subsection and rewriting v_x, v_y in terms of cylindrical velocity coordinates:

$$\begin{aligned} v_x &= v_{\perp}(\tau) \cos[\tau + \varepsilon(\tau)] + \frac{E_y}{B}, \\ v_y &= -v_{\perp}(\tau) \sin[\tau + \varepsilon(\tau)] + \frac{d}{d\tau} \left(\frac{E_y}{B} \right). \end{aligned} \quad (8.69)$$

The variables v_x, v_y have been replaced by new unknowns $v_{\perp}(\tau), \varepsilon(\tau)$. Both the amplitude and phase of the gyro motion are assumed to be functions of time and, in fact, they turn out to be slowly varying functions of time. The form given by Eq. (8.69) already demonstrates the slight modification to the polarization drift in which the B field must be included in the time derivative. The remainder of the analysis focuses on solving for $v_{\perp}(\tau)$ leading to the identification of the new approximate constant of the motion. The solution for $\varepsilon(\tau)$ can also be easily found but no new important information is contained therein and hence the corresponding analysis is suppressed.

To find the solution for $v_{\perp}(\tau)$ one additional step is required before substituting Eq. (8.69) into Eq. (8.68). An expression is required for $x - x_g$ in the velocity equations. Since this expression appears only in the small, expanded term, the leading order gyro motion contribution is all that is required. From the second two trajectory equations in Eq. (8.68) one finds that

$$x - x_g \approx \frac{v_{\perp}(\tau)}{\omega_c(\tau)} \sin[\tau + \varepsilon(\tau)]. \quad (8.70)$$

Equations (8.69) and (8.70) are now substituted into the velocity components of Eq. (8.68). The resulting two equations can easily be solved simultaneously for $dv_{\perp}/d\tau$ and $d\varepsilon/d\tau$. A short calculation yields the desired equation for $v_{\perp}(\tau)$.

$$\frac{dv_{\perp}}{d\tau} + \frac{v_{\perp}}{2\omega_c B} \left[\frac{\partial E_y}{\partial x_g} + \frac{\partial E_y}{\partial x_g} \cos 2(\tau + \varepsilon) \right] = \frac{d^2}{d\tau^2} \left(\frac{E_y}{B} \right) \sin(\tau + \varepsilon) \approx 0. \quad (8.71)$$

As in the previous subsection the term on the right hand side is a higher order iteration correction and can be neglected.

The next step is to simplify Eq. (8.71) by using Faraday's law to replace $\partial E_y/\partial x_g = -dB/dt = -\omega_c dB/d\tau$. Equation (8.71) reduces to

$$\frac{1}{\mu} \frac{d\mu}{d\tau} = \frac{1}{B} \frac{dB}{d\tau} \cos 2(\tau + \varepsilon), \quad (8.72)$$

where

$$\mu \equiv mv_{\perp}^2/2B \quad (8.73)$$

is known as the magnetic moment (for reasons to be discussed shortly). This expression can be further simplified. Upon integrating Eq. (8.72) over one gyro period ($\tau_0 \leq \tau + \varepsilon \leq \tau_0 + 2\pi$), one finds that the right hand side almost exactly averages to zero, except for a very small, negligible correction of order $(\omega/\omega_c)^2$. Thus, to a very high degree of accuracy it follows that $\langle d \ln \mu/d\tau \rangle = 0$. The implication is that μ is a constant of the motion when averaged over one gyro period.

$$\mu = \frac{mv_{\perp}^2(t)}{2B(t)} = \text{const.} \quad (8.74)$$

Significance of μ

The quantity μ is known as the first adiabatic invariant and is equal to the gyro-averaged magnetic moment of the charged particle. This can be easily seen by recalling that the usual definition of the magnetic moment is $\mu = IA$, where I is the current flowing in a circular loop and A is the area of the loop. For a particle gyrating in a magnetic field the current averaged over one gyro period is given by $I = q/\tau_c = q\omega_c/2\pi$, while the area is given by $A = \pi r_L^2 = \pi(mv_{\perp}/qB)^2$. Since the product $IA = mv_{\perp}^2/2B$, the quantity μ is indeed the magnetic moment.

The fact that μ is constant when averaged over a gyro period can be interpreted as follows. The magnetic flux enclosed by a particle over one gyro orbit is just $\psi = \pi r_L^2 B = (\tau\pi m/q^2)\mu \sim \mu$. Therefore, as the B field changes slowly in time the perpendicular velocity and corresponding gyro radius also change slowly in time in such a way that the flux contained within the orbit is a constant.

Summary of generalized results

A charged particle moving in time varying electric and magnetic fields experiences an additional guiding center drift known as the polarization drift. This drift, for $\mathbf{B} = B(t)\mathbf{e}_z$ and the general case $\mathbf{E}_\perp = E_x(\mathbf{r}_\perp, t)\mathbf{e}_x + E_y(\mathbf{r}_\perp, t)\mathbf{e}_y$, follows from Eq. (8.69) and is given by (top sign for electrons)

$$\mathbf{V}_p = \mp \frac{1}{\omega_c} \frac{d}{dt} \left(\frac{\mathbf{E}_\perp}{B} \right). \quad (8.75)$$

The second new result is the identification of an approximate constant of the motion known as the adiabatic invariant. It is only “approximately” a constant since the derivation requires averaging over a gyro period assuming that the magnetic field is varying slowly (i.e., adiabatically). The adiabatic invariant is given by

$$\mu = \frac{mv_\perp^2(t)}{2B(t)} = \text{const.} \quad (8.76)$$

In terms of fusion applications the polarization drift plays an important role in setting the time scale for macroscopic plasma instabilities. As is shown in Chapter 12 which describes macroscopic macroscopic equilibrium and stability, the time scale associated with the polarization drift is very fast compared to experimental times. If a given magnetic configuration is unstable the plasma is rapidly lost to the wall because of the fast time scale. The conclusion is that for fusion the magnetic configurations must be designed to avoid such instabilities.

The adiabatic invariant plays an important role in two different ways. First it is the basis for a magnetic confinement configuration known as the “mirror machine,” which is discussed shortly. Second, the magnetic moment plays an important role in many toroidal magnetic geometries leading to a surprisingly enhanced collisional transport of energy and particles across the magnetic field. This behavior is known as “neoclassical transport theory” and is discussed in Chapter 14. While both of these applications depend on the adiabatic invariant, they are more connected to the result that μ is a constant in slow spatially varying magnetic fields as opposed to slow time varying fields. This spatial result has not as yet been demonstrated but is a major topic in the next section.

8.9 Motion in fields with parallel gradients: the magnetic moment and mirroring

The last topic concerning guiding center motion involves the effect of a parallel gradient in the magnetic field, which can arise in configurations such as those illustrated in Fig. 8.11. Two important results are obtained in the limit where the gyro radius is small compared to the spatial gradient length of the field. First, the quantity $\mu = mv_\perp^2/2B$ is again shown to be an adiabatic invariant. Second, a gyro-averaged force develops parallel to the magnetic field gradient which can have a large impact on the parallel guiding center motion. This force gives rise to the “mirror” effect and provides the basis for one of the earliest

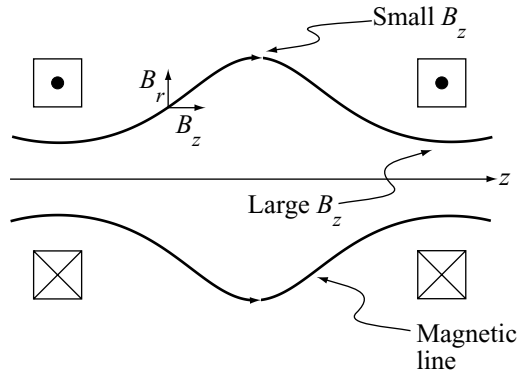


Figure 8.11 Coil configuration giving rise to a parallel gradient in B .

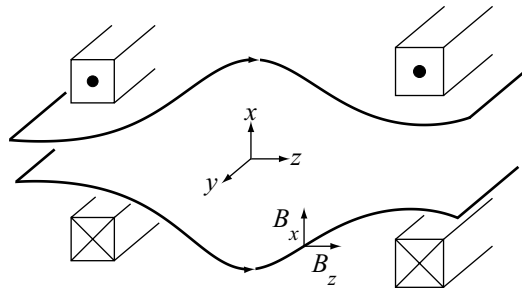


Figure 8.12 Slab model of a magnetic geometry with a parallel gradient.

fusion experiments. The mirror effect and the simple mirror machine are also discussed in this section.

In terms of the mathematics, parallel magnetic field gradients complicate the analysis because the geometry is inherently 2-D. For example, even in the simplest case where $B_z = B_z(z)$, there must be an additional transverse component of \mathbf{B} in order to satisfy $\nabla \cdot \mathbf{B} = 0$. For mathematical tractability in the analysis these transverse components are chosen to satisfy the “long-thin” approximation which assumes that the parallel gradient length is large compared to the transverse gradient length. Although not essential, this approximation greatly simplifies the calculation while still capturing the essential physics.

8.9.1 The mathematical formulation

Consider first the prescribed fields. The electric field is assumed to be zero: $\mathbf{E} = 0$. The magnetic field geometry, for simplicity, is taken to be a slab version of the cylindrical configuration in Fig. 8.11. The slab model is illustrated in Fig. 8.12. The magnetic field is static in time and has the following non-zero components: $\mathbf{B} = B_x(x, z)\mathbf{e}_x + B_z(x, z)\mathbf{e}_z$. For the moment no long-thin approximation is made, implying that $B_x \sim B_z$. Under these

assumptions the equations of motion for the particle velocities become

$$\begin{aligned}\frac{dv_x}{dt} &= \frac{q}{m} v_y B_z, \\ \frac{dv_y}{dt} &= -\frac{q}{m} (v_x B_z - v_z B_x), \\ \frac{dv_z}{dt} &= -\frac{q}{m} v_y B_x.\end{aligned}\tag{8.77}$$

As in earlier calculations these equations will be solved by expansion techniques. A potential difficulty that arises is that the simple coordinate z no longer corresponds to the parallel direction. Thus, while v_z may be nearly the parallel velocity and v_x, v_y the perpendicular velocities they are not exactly so and these deviations introduce a number of small additional terms that compete with the small gyro radius corrections. These geometric complications can be eliminated at the outset by the introduction of a set of three orthogonal unit vectors and corresponding velocity components that exactly distinguish between the perpendicular and parallel directions. The new unit vectors $\mathbf{e}_1, \mathbf{e}_2, \mathbf{b}$, and their inverse relations are given by

$$\begin{aligned}\mathbf{b} &= b_x \mathbf{e}_x + b_z \mathbf{e}_z, & \mathbf{e}_z &= b_z \mathbf{b} - b_x \mathbf{e}_1, \\ \mathbf{e}_2 &= \mathbf{e}_y, & \mathbf{e}_y &= \mathbf{e}_2, \\ \mathbf{e}_1 &= \mathbf{e}_2 \times \mathbf{b} = b_z \mathbf{e}_x - b_x \mathbf{e}_z, & \mathbf{e}_x &= b_z \mathbf{e}_1 + b_x \mathbf{b},\end{aligned}\tag{8.78}$$

where $b_x = B_x/B$ and $b_z = B_z/B$. Observe that \mathbf{b} points along the magnetic field while $\mathbf{e}_1, \mathbf{e}_2$ are exactly perpendicular to \mathbf{B} . The corresponding velocity components v_1, v_2, v_{\parallel} and their inverses can now be written as

$$\begin{aligned}v_{\parallel} &= b_z v_z + b_x v_x, & v_z &= b_z v_{\parallel} - b_x v_1, \\ v_2 &= v_y, & v_y &= v_2, \\ v_1 &= b_z v_x - b_x v_z, & v_x &= b_x v_{\parallel} + b_z v_1.\end{aligned}\tag{8.79}$$

Using these transformations, one can show after a short calculation that the equations of motion are substantially simplified and can be rewritten as follows:

$$\begin{aligned}\frac{dv_1}{dt} - \omega_c v_2 &= K v_{\parallel}, \\ \frac{dv_2}{dt} + \omega_c v_1 &= 0, \\ \frac{dv_{\parallel}}{dt} &= -K v_1,\end{aligned}\tag{8.80}$$

where $\omega_c = qB/m$, $B = (B_x^2 + B_z^2)^{1/2}$ and

$$K = K[x(t), z(t)] = b_x \frac{db_z}{dt} - b_z \frac{db_x}{dt}.\tag{8.81}$$

The equations are now in the desired form.

8.9.2 Solution to the equations

The mathematical solution to the problem requires two steps. First a new time variable is introduced, similar to the transformation used in the generalized polarization drift analysis. Second, an explicit model is introduced for the magnetic field enabling the introduction of the long–thin approximation.

The analysis begins with the time transformation which is given by

$$\tau = \int_0^t \omega_c dt \quad (8.82)$$

with $\omega_c(t) = \omega_c[x(t), z(t)]$. Note that this transformation is formally identical to the one used for the polarization drift (i.e., Eq. (8.67)). However, it is inherently implicit in nature since $x(t), z(t)$ are unknown functions. Even so, as is shown, this does not lead to any difficulties in the analysis. Substituting the transformation into the equations of motion yields

$$\begin{aligned} dv_1/d\tau - v_2 &= \hat{K} v_{\parallel}, \\ dv_2/d\tau + v_1 &= 0, \\ dv_{\parallel}/d\tau &= -\hat{K} v_1, \end{aligned} \quad (8.83)$$

with

$$\hat{K} = K/\omega_c = b_x db_z/d\tau - b_z db_x/d\tau. \quad (8.84)$$

The next step is to introduce an explicit model for the magnetic field. The simplest model containing a parallel field gradient has the form $B_z = B_z(z)$. Perpendicular gradients in B_z have already been discussed, are not necessary for the present calculation, and are thus not included. The condition that $\nabla \cdot \mathbf{B} = 0$ requires the existence of a non-zero transverse magnetic field. For the slab geometry under consideration this implies a non-zero $B_x(x, z)$. A simple calculation then shows that the explicit magnetic field under consideration is given by

$$\begin{aligned} B_z &= B_z(z), \\ B_x &= -x dB_z/dz. \end{aligned} \quad (8.85)$$

It is now straightforward to introduce the long–thin approximation into the model. The primary motivation for introducing the approximation is to obtain a simplified expression for \hat{K} . One assumes that the transverse scale of the configuration is characterized by $x \sim a$ and that the parallel gradient length is defined by $B'_z/B_z \sim 1/L$. The long–thin approximation requires that $a/L \ll 1$ and implies that $B_x/B_z \sim a/L \ll 1$.

After a short calculation one can show that substitution of the model magnetic field and the long–thin approximation results in the following leading order contribution to \hat{K} :

$$\begin{aligned} \hat{K} &= b_x \frac{db_z}{d\tau} - b_z \frac{db_x}{d\tau} = \frac{B_z^2}{B^2} \frac{d}{d\tau} \left(\frac{x}{B_z} \frac{dB_z}{dz} \right) \approx \frac{dx}{d\tau} \left(\frac{1}{B_z} \frac{dB_z}{dz} \right) \\ &\approx \frac{v_1}{\omega_c B_z} \frac{dB_z}{dz} \approx \frac{v_1}{v_{\parallel} B_z} \frac{dB_z}{d\tau}. \end{aligned} \quad (8.86)$$

In the last two expressions z and τ are used interchangeably as independent variables by the one-to-one implicit relationship $dz = (v_z/\omega_c)d\tau \approx (v_{\parallel}/\omega_c)d\tau$. Note that there are many more terms contributing to Eq. (8.86) but they are all smaller by at least a/L or r_L/a .

It is now straightforward to solve the equations. Consider first, the adiabatic invariant. As in the analysis of the generalized polarization drift it is useful to introduce cylindrical velocity variables with slowly varying coefficients:

$$\begin{aligned} v_1 &= v_{\perp}(\tau)\cos[\tau + \varepsilon(\tau)], \\ v_2 &= -v_{\perp}(\tau)\sin[\tau + \varepsilon(\tau)]. \end{aligned} \quad (8.87)$$

One substitutes into the perpendicular components of the equations of motion obtaining a set of simultaneous equations for \dot{v}_{\perp} and $\dot{\varepsilon}$. The unknown $\dot{\varepsilon}$ can easily be eliminated yielding the following equation for \dot{v}_{\perp} :

$$\frac{dv_{\perp}}{d\tau} = \frac{v_{\perp}}{2B_z} \frac{dB_z}{d\tau} [1 + \cos 2(\tau + \varepsilon)], \quad (8.88)$$

which can straightforwardly be rewritten as

$$\frac{1}{\mu} \frac{d\mu}{d\tau} = \left(\frac{1}{B_z} \frac{dB_z}{d\tau} \right) \cos 2(\tau + \varepsilon). \quad (8.89)$$

After averaging over a gyro period one again finds that

$$\mu = \frac{mv_{\perp}^2(z)}{2B(z)} = \text{const.} \quad (8.90)$$

The quantity μ is an adiabatic invariant, although in this case for a slow spatially rather than time varying magnetic field.

The second part of the mathematical solution involves the parallel component of the equations of motion which in the long–thin approximation reduces to

$$\frac{dv_{\parallel}}{d\tau} = -\frac{v_{\perp}^2}{\omega_c B_z} \frac{dB_z}{dz} = -\frac{v_{\perp}^2}{2\omega_c B_z} \frac{dB_z}{dz} [1 + \cos(\tau + \varepsilon)]. \quad (8.91)$$

After averaging over the gyro motion and converting back to the real time independent variable, one can rewrite this expression as

$$m \frac{dv_{\parallel}}{dt} = -\mu \frac{dB_z}{dz} = -\mu \nabla_{\parallel} B. \quad (8.92)$$

Observe that there is a gyro-averaged force acting on the parallel guiding center motion of the particle. The force is driven by the parallel gradient in the magnetic field. Two forms are given for the force. The first is the direct result of the calculation, while the second is a generalization that does not make use of the long–thin approximation.

At this point one might think that a paradox has arisen. It has been shown in Section 8.2 that the parallel magnetic force acting on a charged particle is exactly and instantaneously zero. How then can there be an average force parallel to the magnetic field as derived above in Eq. (8.92)? The answer is subtle and can be understood by examining Fig. 8.13, which shows a particle with perpendicular velocity v_{\perp} gyrating around a magnetic line in a field with a parallel gradient. The key point is that when $v_{\perp} \neq 0$, the particle has a finite gyro

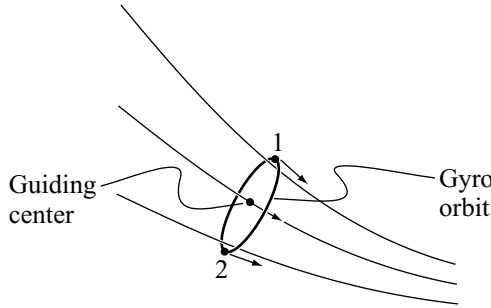


Figure 8.13 Comparison of field directions between the guiding center and the actual particle trajectory (point 1 steeper and point 2 shallower).

radius which produces a small excursion of the orbit (i.e., gyro motion) perpendicular to the guiding center trajectory. Observe that as the particle gyrates, the top of the orbit (point 1) lies on a magnetic line that is slightly steeper than the magnetic line of the guiding center. Similarly, at the bottom of the orbit (point 2) the particle lies on a shallower magnetic line. To leading order the steepness and shallowness average out and the average parallel motion of the particle is parallel to the guiding center. However, to first order the cancellation is not perfect and there is a small correction leading to the “parallel” force given by Eq. (8.92).

The resolution of the paradox can thus be summarized as follows. In a magnetic field with a parallel gradient there is indeed an average parallel force acting on the guiding center motion of the particle. It should be emphasized that the force acts at the guiding center and not the instantaneous position of the particle. Furthermore, the direction of the field at the guiding center is slightly different from the average direction of the actual field experienced by the particle as it gyrates along its orbit. In other words, the field at the guiding center is not exactly parallel to the actual average field experienced by the particle. Therefore, while the guiding center motion feels a parallel force along the gradient, this force is actually in the perpendicular direction when viewed in terms of the instantaneous position of the particle.

In conclusion a parallel magnetic field gradient produces a force that acts on the parallel guiding center motion of the particle. This force produces an important mirroring effect on the particles which is the topic of the next subsection.

8.9.3 The mirror effect and the mirror machine

The combination of $\mu = \text{const.}$ and $F_{\parallel} = -\mu \nabla_{\parallel} B$ can have a dramatic impact on the parallel motion of the guiding center. In particular, the direction of the parallel motion can be completely reversed so that a particle moving to the right along a given field line at a certain instant of time can be moving to the left a short time later. In fact there is a critical

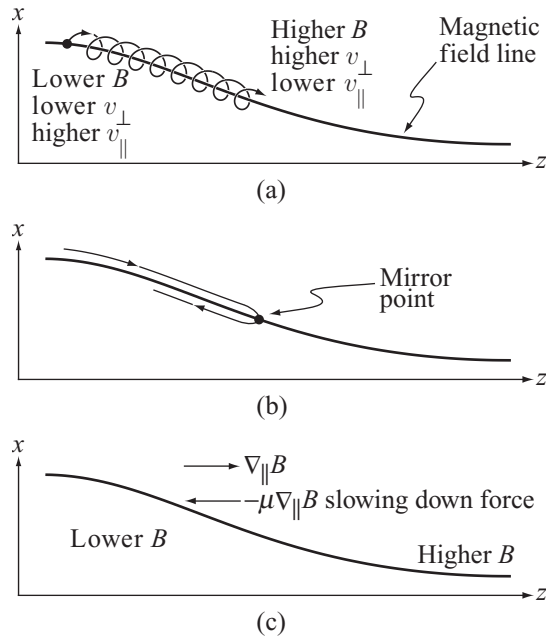


Figure 8.14 The mirror effect (a) as a particle moves into a region of higher B , v_{\perp} increases and v_{\parallel} decreases; (b) parallel guiding center velocity reflected at the mirror point where $v_{\parallel} = 0$; (c) the parallel guiding center force.

point along the trajectory where the particle is reflected. Not surprisingly, this point is called the “mirror point” and the whole reversal process, the “mirror effect.”

A qualitative picture of the mirror effect

The phenomenon of mirroring can be understood qualitatively by examining Fig. 8.14. The trajectory of a particle moving to the right into a region of higher magnetic field is shown in Fig. 8.14(a). The particle starts off in a region of lower field with a certain value of v_{\perp} and v_{\parallel} . As the particle gyrates and moves parallel to \mathbf{B} into the high-field region, the value of B along the guiding center increases. Since $\mu = mv_{\perp}^2/2B = \text{const.}$ this implies that v_{\perp} must also increase. Next, recall that in a static magnetic field the kinetic energy of a particle is an exact constant of the motion: $E = m(v_{\perp}^2 + v_{\parallel}^2)/2 = \text{const.}$ Consequently, an increase in v_{\perp} must be accompanied by a decrease in v_{\parallel} . If the increase in B is sufficiently large, the particle eventually reaches a point along its trajectory where $v_{\parallel} = 0$. This is the reflection point as shown in Fig. 8.14(b). Once reflected, the parallel velocity of the particle reverses direction and the guiding center motion starts moving to the left. The force causing this behavior of the parallel motion is just $F_{\parallel} = -\mu \nabla_{\parallel} B$. As can be seen in Fig. 8.14(c) it acts to slow down parallel guiding center motion as a particle enters a high-field region.

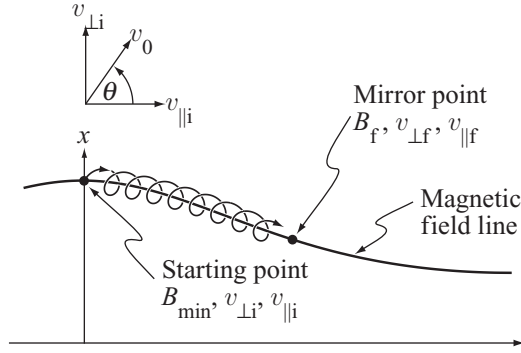


Figure 8.15 Conditions for reflecting a particle at the mirror point $B = B_f$.

The quantitative conditions for mirroring

The conditions for mirroring to occur can easily be quantified using the constants of the motion μ and E . The goal of the calculation is to determine the relation between v_{\perp} and v_{\parallel} necessary to reflect a particle at a given point along the parallel field gradient. To begin, consider a particle moving in a mirror field as illustrated in Fig. 8.15. Assume the particle starts initially at the midplane, where the magnetic field is weakest. At this point $B = B_{\min}$, $v_{\perp} = v_{\perp i}$, $v_{\parallel} = v_{\parallel i}$. The corresponding magnetic moment and energy are given by $\mu = mv_{\perp i}^2/2B_{\min}$ and $E = m(v_{\perp i}^2 + v_{\parallel i}^2)/2$.

Assume now that the particle moves to the right and is reflected at the point where $B = B_f > B_{\min}$. At this point $v_{\perp} = v_{\perp f}$ and by definition of the reflection point $v_{\parallel} = v_{\parallel f} = 0$. The corresponding energy and magnetic moment then have the values $E = mv_{\perp f}^2/2$ and $\mu = mv_{\perp f}^2/2B_f$.

The reflection condition can now be easily calculated by equating the initial and final values of E and μ . To proceed it is convenient to define a normalized energy $E = mv_0^2/2$. The initial velocity can then be expressed in terms of a pitch angle θ as follows (see Fig. 8.15):

$$\begin{aligned} v_{\perp i} &= v_0 \sin \theta, \\ v_{\parallel i} &= v_0 \cos \theta. \end{aligned} \quad (8.93)$$

Conservation of energy clearly implies that

$$v_{\perp f}^2 = v_{\perp i}^2 + v_{\parallel i}^2 = v_0^2. \quad (8.94)$$

Next conservation of μ is applied leading to

$$\frac{v_{\perp i}^2}{B_{\min}} = \frac{v_{\perp f}^2}{B_f}, \quad (8.95)$$

which simplifies to

$$\sin^2 \theta_c = \frac{B_{\min}}{B_f}. \quad (8.96)$$

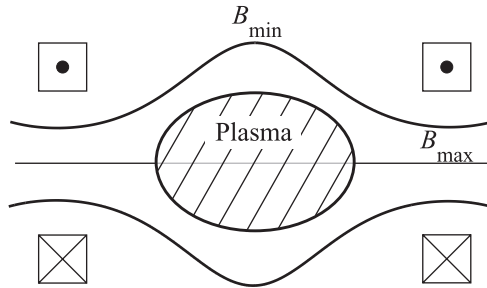


Figure 8.16 Geometry of the simple mirror machine.

Here, $\theta = \theta_c$ is the critical pitch angle for mirror reflection at the point where $B = B_f$. A particle with a higher initial perpendicular velocity, corresponding to a pitch angle $\theta > \theta_c$, will be reflected sooner. Conversely, a particle with a smaller initial perpendicular velocity, $\theta < \theta_c$, will pass the point where $B = B_f$ and may or may not be reflected later, depending upon how large the magnetic field becomes.

In summary, the analysis has shown that for a given parallel gradient in the magnetic field, it is easier to reflect particles with a large pitch angle (i.e., high perpendicular and low parallel initial velocities).

The simple mirror machine

The mirror effect just described forms the basis for one of the earliest magnetic fusion configurations, appropriately known as the “mirror machine.” Its simplest form is illustrated in Fig. 8.16. Two coils with current flowing in the same direction create a magnetic field with a maximum just under each coil and a local minimum midway between. Assume now that plasma initially fills the volume between the coils. Using the guiding center theory of the mirror effect one wishes to determine which, if any, particles remain confined in the prescribed magnetic geometry. Within the context of the theory, it is shown that a large fraction of the particles remain confined, and this fact provided the motivation for the early consideration of the mirror machine as a fusion device.

The analysis is straightforward. Particles with a sufficiently large pitch angle (i.e., large v_{\perp}/v_{\parallel}) at the center of the configuration where $B = B_{\min}$ reflect off the mirror point somewhere along the gradient where $B = B_f$. The particle with the smallest initial pitch angle that is still reflected is the one that is reflected at the mirror throat where $B = B_{\max}$. The corresponding critical pitch angle is given by

$$\sin^2 \theta_c = \frac{B_{\min}}{B_{\max}} \equiv \frac{1}{R}. \quad (8.97)$$

Here, $R = B_{\max}/B_{\min} > 1$ is defined as the mirror ratio. Particles with a pitch angle $\theta > \theta_c$ (i.e., a high v_{\perp}) will be reflected sooner, before reaching the mirror throat. These particles then reverse direction and reflect off the opposite mirror. In this way, the particles remain

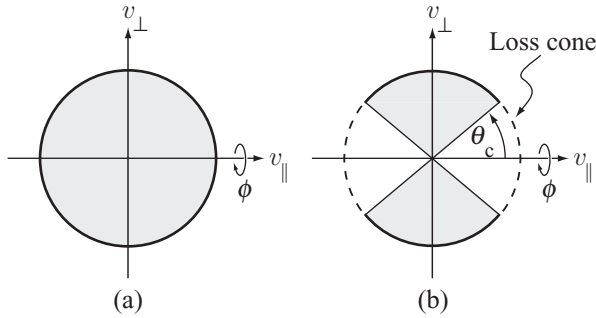


Figure 8.17 Velocity phase space showing: (a) a full, isotropic Maxwellian and (b) a Maxwellian with a loss cone.

confined indefinitely, continually bouncing between mirror reflection points. In contrast, particles with $\theta < \theta_c$ (i.e., a high v_{\parallel}) pass the mirror throat without being reflected. They are quickly lost to the first wall.

This analysis shows that the subset of particles confined in a mirror machine is defined by the range of pitch angles

$$\theta_c \leq \theta \leq \pi - \theta_c. \quad (8.98)$$

Pitch angles outside this range form a “loss cone” in velocity space in which all the particles have been lost. The concept of the loss cone is illustrated in Fig. 8.17, which depicts the density of particles in v_{\perp} , v_{\parallel} , ϕ space. Figure 8.17(a) corresponds to an isotropic distribution function such as a Maxwellian, with no loss cone. The shaded region represents a sphere with a uniform distribution of particles. Figure 8.17(b) shows the effect of losing particles with a small pitch angle. A cone of particles is removed from opposite poles of a sphere and only the remaining shaded region contains mirror confined particles.

The fraction of confined particles f of an initially Maxwellian distribution function $F_M(v)$ is equal to the ratio of the number of particles outside the loss cone divided by the total number of particles. This fraction is easily calculated in terms of the mirror ratio as follows:

$$\begin{aligned} f &= \frac{\int_{\theta_c}^{\pi-\theta_c} \sin \theta \, d\theta \int_0^{2\pi} d\phi \int_0^{2\pi} v^2 F_M(v) \, dv}{\int_0^{\pi} \sin \theta \, d\theta \int_0^{2\pi} d\phi \int_0^{2\pi} v^2 F_M(v) \, dv} \\ &= \frac{\int_{\theta_c}^{\pi-\theta_c} \sin \theta \, d\theta}{\int_0^{\pi} \sin \theta \, d\theta} = \left(1 - \frac{1}{R}\right)^{1/2}. \end{aligned} \quad (8.99)$$

Observe that for a mirror ratio $R = 2$, about 70% of the particles are confined, quite a substantial fraction.

In practical experiments, the simple mirror machine did not work as well as predicted. Both macroscopic and microscopic instabilities were observed, leading to anomalously fast losses of particles. Careful analysis and several very clever ideas ultimately were able to mitigate these effects. However, there still remained one irreducible problem. Coulomb collisions scattered confined particles into the loss cone, after which they were immediately lost out of the ends of the device. The rate at which particles were lost was just too fast to achieve a favorable power balance in a mirror machine fusion reactor. This topic will be revisited in more detail after the discussion of Coulomb collisions in the next chapter.

8.10 Summary – putting all the pieces together

This chapter has described the motion of a charged particle in a prescribed set of smooth magnetic and electric fields. A wide choice of fields has been investigated allowing for perpendicular and parallel spatial gradients as well as time variation. A useful intuition has been developed by assuming that the spatial gradient length is long compared to the gyro radius and the characteristic frequency associated with the time variation is low compared to the gyro frequency. This is very often the situation of practical importance.

The analysis has shown that the perpendicular particle motion can be decomposed into two components: the fast gyro motion and the slower guiding center motion comprising primarily the guiding center drifts. In the parallel direction, only guiding center motion is important. Thus, the trajectory of a particle can be accurately approximated by

$$\begin{aligned}\mathbf{v}(t) &= \mathbf{v}_{\text{gyro}} + \mathbf{v}_g + v_{\parallel} \mathbf{b}, \\ \mathbf{r}(t) &= \mathbf{r}_{\text{gyro}} + \mathbf{r}_g + l \mathbf{b}.\end{aligned}\tag{8.100}$$

The velocity and position are given in terms of the magnetic and electric fields, which are assumed to be of the form

$$\begin{aligned}\mathbf{B} &= B(\mathbf{r}, t) \mathbf{b}, \\ \mathbf{E} &= \mathbf{E}_{\perp}(\mathbf{r}, t) + E_{\parallel}(\mathbf{r}, t) \mathbf{b}.\end{aligned}\tag{8.101}$$

The gyro motion, expressed in terms of a local perpendicular, rectangular coordinate system whose axis corresponds to the guiding center of the particle, is given by

$$\begin{aligned}\mathbf{v}_{\text{gyro}} &= v_{\perp} \cos \tau \mathbf{e}_x \pm v_{\perp} \sin \tau \mathbf{e}_y, \\ \mathbf{r}_{\text{gyro}} &= r_L \sin \tau \mathbf{e}_x \mp r_L \cos \tau \mathbf{e}_y.\end{aligned}\tag{8.102}$$

where the upper sign here and below corresponds to electrons, $r_L = v_{\perp}/\omega_c$, $\omega_c = |q|B(\mathbf{r}_g, l, t)/m$, and

$$\tau = \int_0^t \omega_c(\mathbf{r}_g, l, t) dt.\tag{8.103}$$

In these expressions v_{\perp} , \mathbf{r}_g , l are slowly varying functions of time determined from the solution of the guiding center trajectories.

The guiding center motion is described by a closed set of equations for the unknowns v_{\perp} , \mathbf{v}_g , v_{\parallel} , \mathbf{r}_g , l . Also, each guiding center particle is characterized by a magnetic moment μ as well as a charge q and mass m , all of which are assumed to be known quantities. Consider first the perpendicular guiding center drift velocity, which comprises the following contributions:

$$\mathbf{v}_g = \mathbf{V}_E + \mathbf{V}_{\nabla B} + \mathbf{V}_{\kappa} + \mathbf{V}_p. \quad (8.104)$$

The individual drift velocities, expressed in terms of the local rectangular coordinate system ($\mathbf{r}_g = x_g \mathbf{e}_x + y_g \mathbf{e}_y$) can be written as

$$\begin{aligned} \mathbf{V}_E &= \frac{\mathbf{E}_{\perp} \times \mathbf{B}}{B^2} \quad \mathbf{E} \times \mathbf{B} \text{ drift,} \\ \mathbf{V}_{\nabla B} &= \mp \frac{v_{\perp}^2}{2\omega_c} \frac{\mathbf{B} \times \nabla B}{B^2} \quad \nabla B \text{ drift,} \\ \mathbf{V}_{\kappa} &= \mp \frac{v_{\parallel}^2}{\omega_c} \frac{\mathbf{R}_c \times \mathbf{B}}{R_c^2 B} \quad \text{curvature drift,} \\ \mathbf{V}_p &= \mp \frac{1}{\omega_c} \mathbf{b} \times \frac{d\mathbf{V}_E}{dt} \quad \text{polarization drift,} \end{aligned} \quad (8.105)$$

Here and below, all fields are evaluated at the guiding center.

The perpendicular velocity is expressed in terms of the adiabatic invariant

$$v_{\perp}^2 = 2\mu B/m, \quad (8.106)$$

while the parallel velocity is obtained by solving the differential equation

$$m \frac{dv_{\parallel}}{dt} = qE_{\parallel} - \mu \frac{\partial B}{\partial l}. \quad (8.107)$$

Finally, the guiding center position is obtained by solving

$$\begin{aligned} d\mathbf{r}_g/dt &= \mathbf{v}_g, \\ dl/dt &= v_{\parallel}. \end{aligned} \quad (8.108)$$

Equations (8.104)–(8.108) form a closed set of coupled ordinary differential equations for determining the guiding center motion. Often when the fields are static or possess geometric symmetry one can solve the equations analytically. Qualitatively, the guiding center motion represents the gyro-averaged trajectory of the particle. In the perpendicular direction the motion consists of the combination of drifts given above. In the parallel direction the velocity is determined by: (1) the parallel gradient in the magnetic field coupled with the fact that μ is an adiabatic invariant, as well as (2) the parallel electric field if one exists. Focusing on the guiding center motion often provides a much better intuition of plasma behavior than

examining the details of the exact particle trajectory. This intuition, as will be shown, is of great help in understanding the confinement of fusion plasmas.

Bibliography

Single-particle motion in magnetic and electric fields has many applications including fusion, space plasma physics, and astrophysics. Various treatments appear in the literature, some simple and intuitive, others more formal and rigorous. Most treatments focus on deriving the guiding center motion of charged particles, ignoring collisions, and assuming slow variation in the length and time scale of the applied fields. Several references for additional reading are listed below.

- Boyd, T. J. M. and Sanderson, J. J. (2003). *The Physics of Plasmas*. Cambridge, England: Cambridge University Press.
- Chen, F. F. (1984). *Introduction to Plasma Physics and Controlled Fusion*, second edn. New York: Plenum Press.
- Dolan, T. J. (1982). *Fusion Research*. New York: Pergamon Press.
- Goldston, R. J. and Rutherford, P. H. (1995). *Introduction to Plasma Physics*. Bristol, England: Institute of Physics Publishing.
- Helander, P. and Sigmar, D. J. (2002). *Collisional Transport in Magnetized Plasmas*. Cambridge, England: Cambridge University Press.
- Miyamoto, K. (2001). *Fundamentals of Plasma Physics and Controlled Fusion*, revised edn. Toki City: National Institute for Fusion Science.
- Northrup, T. G. (1966). *Adiabatic Charged particle Motion* (Kunkel, W. B. editor). New York: McGraw Hill Book Company.
- Stacey, W. M. (2005). *Fusion Plasma Physics*. Weinheim: Wiley-VCH.
- Wesson, J. (2004). *Tokamaks*. third edn. Oxford: Oxford University Press.

Problems

- 8.1 Consider a plasma with azimuthal symmetry: $\partial/\partial\theta = 0$. Express the fields in terms of a scalar potential $\phi(r, z, t)$ and vector potential $\mathbf{A}(r, z, t)$. Form the dot product of the single-particle momentum equation with the \mathbf{e}_θ vector. Show that the canonical angular momentum $p_\theta = mrv_\theta + q\psi$ is an exact constant of the motion. Here, $\psi = rA_\theta$.
- 8.2 This problem investigates several points arising in connection with the derivation of the ∇B drift. Specifically, the calculation in the text is generalized to a 2-D magnetic field and the consequences of the second harmonic terms appearing in the derivation are investigated.
- (a) Consider a magnetic field of the form $\mathbf{B} = B(x, y)\mathbf{e}_z$. Taylor expand about the guiding center position in both the x and the y direction. Following the derivation in section 8.5.1 show that the general form of the ∇B drift is given by

$$\mathbf{V}_{\nabla B} = \mp \frac{v_\perp^2}{2\omega_c} \frac{\mathbf{B} \times \nabla B}{B^2}.$$

- (b) Next, consider the contributions due to the second harmonic terms. Find the first order corrections to both the particle velocity and position by calculating a particular solution to the equations and then satisfying the initial conditions by an

appropriate choice of homogeneous solution. Show that the modified trajectory remains circular but with a slightly different location for the guiding center and a slightly modified size for the gyro radius as given by the primed quantities below:

$$\begin{aligned} r_L'^2 &= r_L^2 \left(1 + \frac{\mathbf{v}_{\perp 0} \cdot \mathbf{B} \times \nabla B}{\omega_c B^2} \right), \\ \mathbf{r}'_g &= \mathbf{r}_g - \frac{\mathbf{v}_{\perp 0} \times (\mathbf{v}_{\perp 0} \times \nabla B)}{2\omega_c^2 B}, \\ \mathbf{v}_{\perp 0} &= v_{\perp} (\mathbf{e}_x \cos \phi + \mathbf{e}_y \sin \phi). \end{aligned}$$

Note: The algebra involved in part (b) is straightforward but somewhat tedious.

- 8.3 This problem involves calculating the *second* order corrections to the guiding center motion assuming a uniform magnetic field and an electric field with a perpendicular gradient. Of particular interest is the derivation of the second order “finite gyro radius” drift. Assume the fields are given by $\mathbf{B} = B \mathbf{e}_z$ with $B = \text{const.}$ and $\mathbf{E} = -\nabla \Phi(x, y)$. Expand the equations including all second order terms.

(a) Calculate the generalized corrections to the gyro frequency by assuming that

$$\begin{aligned} v_x &= -\frac{1}{B} \frac{\partial \Phi}{\partial y_g} + v_{\perp} \cos \Omega t + a_1 \sin \Omega t + v_{2x}(t), \\ v_y &= +\frac{1}{B} \frac{\partial \Phi}{\partial x_g} + c_1 \sin \Omega t + v_{2y}(t). \end{aligned}$$

Note the implied special choice of initial conditions to make the problem slightly simpler. Find a_1 and c_1 and show that the generalized shift in gyro frequency, correct to second order in r_L/a , is given by

$$\Omega^2 \approx \omega_c^2 \mp \omega_c \frac{\nabla^2 \Phi}{B} + \frac{1}{B^2} \left[\left(\frac{\partial^2 \Phi}{\partial x \partial y} \right)^2 - \left(\frac{\partial^2 \Phi}{\partial x^2} \right) \left(\frac{\partial^2 \Phi}{\partial y^2} \right) \right] + \dots$$

- (b) Show that the dominant contribution to the second order velocity $\mathbf{v}_2(t)$ is the finite gyro radius drift. The total drift thus can be written as

$$\mathbf{V}_D = - \left(1 + \frac{r_L^2}{4} \nabla^2 \right) \frac{\nabla \Phi \times \mathbf{B}}{B^2}.$$

- 8.4 A 1-D magnetic field with a reversal at the origin can be modeled in a slab geometry by $\mathbf{B} = B_0 \tanh(x/a) \mathbf{e}_z$ with $-\infty < x < \infty$.

- (a) Why are the guiding center formulas for the particle drifts derived in the text invalid?
 (b) Sketch the orbit of a proton with initial conditions $x(0) = y(0) = \dot{y}(0) = 0$ and $\dot{x}(0) = v_{\perp}$.
 (c) Expand about $x = 0$ and derive an expression for the turning point of the orbit x_{max} . Show that $x_{\text{max}} = C r_L^{\alpha} a^{\beta}$, where $r_L = m v_{\perp} / e B_0$. Find C, α, β .

- 8.5 A cylindrical plasma is immersed in a longitudinal magnetic field given by $\mathbf{B} = B_0 [1 - \beta_0 \exp(-r^2/a^2)] \mathbf{e}_z$. For $B_0 = 6 \text{ T}$, $\beta_0 = 0.75$, and $T_e = T_i = 1 \text{ keV}$:

- (a) Calculate the electron and ion gyro frequency and average thermal gyro radius at $r = a$;
 (b) Calculate the magnitude and sign of the electron and ion ∇B drifts at $r = a$;

- (c) Are the guiding center assumptions $r_{Le}/a \ll 1$, $r_{Li}/a \ll 1$, $V_{\nabla B}/v_{\perp} \ll 1$ satisfied?
 - (d) Calculate the direction and sign of the macroscopic current required to produce the dip in the B_z field. Is this compatible with step (b)? Explain.
- 8.6 A plasma has a constant uniform magnetic field $\mathbf{B} = B_0 \mathbf{e}_z$. Superimposed is an electrostatic electric field of the form $\mathbf{E} = E_0 \cos(\omega t - kz) \mathbf{e}_z$, where ω and k are known constants. Assume a positively charged particle is initially located at $z(0) = 0$ with a parallel velocity $v_z(0) = v_{\parallel}$. Show that for a sufficiently large value of E_0 the particle is trapped in the wave. Calculate the critical E_0 .
- 8.7 This problem involves a generalization of the previous electrostatic trapping problem. Consider a positively charged particle acted upon by a magnetic field $\mathbf{B} = B_0 \cos(ky - \omega t) \mathbf{e}_x$.

- (a) Prove that the electric field is given by

$$\mathbf{E} = -(\omega B_0/k) \cos(ky - \omega t) \mathbf{e}_z.$$

- (b) The trajectory of the particle is defined as $\mathbf{r}(t) = x(t) \mathbf{e}_x + y(t) \mathbf{e}_y$. The initial position and velocity of the particle are as follows: $\dot{y}(0) = v_0$ and $y(0) = x(0) = \dot{x}(0) = 0$. Derive a pair of coupled differential equations for $x(t)$ and $y(t)$. One equation should be integrable with the result then substituted into the other equation. The final result should be a single, second order, differential equation involving only one dependent variable. The goal of this part of the problem is to derive this equation.
 - (c) Derive a relationship between v_0 , ω , k , B_0 that defines the boundary between trapped and untrapped particles.
- 8.8 The magnetic field due to an infinitely long wire carrying a current I is given by $\mathbf{B} = (\mu_0 I / 2\pi R) \mathbf{e}_{\phi}$, where ϕ is the toroidal angle.
- (a) Explain why this configuration is not able to successfully confine individual electrons and ions in the R, Z plane.
 - (b) As an extreme example calculate how long it would take for a 10 keV ion to escape from a toroidal chamber whose minor radius is $b = 0.1$ m if the particle is initially located at $R = R_0 = 100$ m, $Z = 0$.

- 8.9 This problem has a somewhat unintuitive answer. Consider the motion of a charged particle in combined magnetic and electric fields $\mathbf{B} = B_0 \mathbf{e}_z$ and $\mathbf{E} = -\nabla \phi$ with $\phi(x, y) = Kxy$. The goal is to find the exact orbit of the particle.

- (a) Write down the exact equations of motion for the trajectory $x(t)$, $y(t)$ of a positively charged particle. These equations should have the form of two coupled second order ODEs. For convenience define $K = \varepsilon e B_0^2 / m$, where ε is an equivalent parameter representing the normalized electric field.
- (b) Find the general solution to the equations. For simplicity assume ε , is small but finite. Describe the qualitative behavior of the orbit for large time.

- 8.10 A positive ion is situated in a uniform magnetic field $\mathbf{B} = B_0 \mathbf{e}_z$. A time varying, spatially uniform electric field is applied of the form $\mathbf{E} = E_0(1 - e^{-t/\tau}) \mathbf{e}_x$.

- (a) Calculate the exact perpendicular velocity of the particle for an ion with the following initial conditions: $v_x(0) = 0$ and $v_y(0) = v_{\perp}$.
- (b) Calculate the guiding center velocity $\mathbf{v}_g(t')$ in the limit $\varepsilon \equiv 1/\omega_c \tau \ll 1$ by averaging over one gyro period as follows:

$$\mathbf{v}_g(t') = \frac{\omega_c}{2\pi} \int_{t'}^{t'+2\pi/\omega_c} \mathbf{v}(t) dt.$$

Are there any transient or steady state guiding center drifts in the x or y direction?

- 8.11 Draw a picture of the earth and its dipole magnetic field. Describe and calculate the orbit of an electron starting off at the equatorial plane with $v_{\parallel} \gg v_{\perp}$. Repeat for an electron with $v_{\parallel} \ll v_{\perp}$.
- 8.12 Consider a hollow cylindrical copper tube. Along the axis is a copper wire. A current I flows in the wire and a low-frequency AC voltage is applied across the tube and the wire.
- Sketch the electric and magnetic fields as a function of r . For simplicity ignore the AC magnetic field.
 - Describe and calculate the orbit of a typical electron and ion placed in this combined magnetic and electric field.
- 8.13 A positive ion is placed in a sheared magnetic field given by

$$\mathbf{B} = B_0[\mathbf{e}_z + (x/L)\mathbf{e}_y].$$

- Write down the exact equations of motion describing the orbit of the particle.
 - Find a relation between $v_z(t)$ and $x(t)$ assuming the following initial conditions: $v_y(0) = v_z(0) = x(0) = y(0) = z(0) = 0$ and $v_x(0) = v_0$.
 - Using this relation derive a single, second order ODE for $x(t)$.
 - Calculate the x location of the turning point of the orbit.
- 8.14 An ion in a cylindrical plasma column moves under the action of a combined magnetic field and electric potential given by $\mathbf{B} = B_0\mathbf{e}_z$ and $\phi = \phi_0(r/a)^2$. Assume that at $t = 0$ the particle passes through the origin $r(0) = 0$ with a velocity $\dot{r}(0) = (2T_i/m_i)^{1/2}$. Calculate and sketch the exact trajectory of the ion as a function of time for various positive values of the parameter $\alpha = \phi_0/a^2 B_0\omega_{ci}$. Can the radial extent of the orbit ever be much smaller than an ion gyro radius? Explain.
- 8.15 In a simple, azimuthally symmetric ($\partial/\partial\theta = 0$) mirror machine, the magnitude of the longitudinal magnetic field near the axis is approximately given by $B_z(r, z) \approx B_0(1 + z^2/L^2)$. Here L is a constant and $z = 0$ is the reflection plane of symmetry.
- Evaluate the magnitude and direction of the curvature vector $\kappa = \mathbf{b} \cdot \nabla\mathbf{b}$ as a function of r, z for small but finite values of r .
 - A mirror trapped ion with total kinetic energy $mv^2/2$ is reflected at the point where $|B| = 2B_0$. Find the particle's v_{\parallel} at the point $z = 0, r = r_0$.
 - Calculate the magnitude and direction of the guiding center drift velocity at $z = 0, r = r_0$.